A quantitative phase-field model for void evolution in defect supersaturated environments: a novel introduction of defect reaction asymmetry

Sreekar Rayaprolu[a], Kyle Starkey[b], Anter El-Azab[a]

[a] School of Materials Engineering, Purdue University, West Lafayette, IN 47907, USA

[b] Currently with Materials Design, Inc.

Abstract

Voids develop in crystalline materials under energetic particle irradiation, as in nuclear reactors. Understanding the underlying mechanisms of void nucleation and growth is of utmost importance as it leads to dimensional instability of the metallic materials. In the past two decades, researchers have adopted the phase-field approach to study the phenomena of void evolution under irradiation. The approach involves modeling the boundary between the void and matrix with a diffused interface. However, none of the existing models are quantitative in nature. This work introduces a thermodynamically consistent, quantitative diffuse interface model based on KKS formalism to describe the void evolution under irradiation. The model concurrently considers both vacancies and self-interstitials in the description of void evolution. Unique to our model is the presence of two mobility parameters in the equation of motion of the phase-field variable. The two mobility parameters relate the driving force for vacancy and self-interstitial interaction to the interface motion, analogous to dislocation motion through climb and glide processes. The asymptotic matching of the phase-field model with the sharp-interface theory fixes the two mobility parameters in terms of the material parameters in the sharp-interface model. The Landau coefficient, which controls the height of the double-well function in the phase field variable, and the gradient coefficient of the phase field variable are fixed based on the interfacial energy and interface width of the boundary. With all the parameters in the model determined in terms of the material parameters, we thus have a new phase field model for void evolution. Simple test cases will show the void evolution under various defect supersaturation to validate our new phase-field model.

I. Introduction

Crystalline materials possess an orderly arrangement of atoms. However, this structured distribution of atoms gets disrupted in the presence of defects. There are several types of defects observed in crystalline materials. For example, zero-dimensional defects like vacancies and self-interstitials; dislocations, the one-dimensional defect; two-dimensional defects like faulted dislocation loops, unfaulted dislocations loops, and stacking faults; finally, three-dimensional defects like voids, bubbles, inclusions, precipitates, stacking fault tetrahedrons. But, in this study, we focus on the evolution of the voids in single-crystalline crystals. The nucleation and growth of voids occur in an environment enriched with vacancies. There exist several scenarios where the conditions become favorable for the nucleation and growth of voids: crystalline materials subjected to irradiation will develop vacancies which diffuse and coalesce into voids [1–4]; in the thin film interconnects of the microelectronic devices whose evolution is governed by the presence of the residual stresses, high current density, and temperature gradients [5–9]; in metallic specimens subjected to tensile deformation [10,11]; in additively manufactured parts creating a material distribution with cavities [12]. These three-dimensional vacancy agglomerates have a detrimental influence on the properties of the metals. For example, the nucleation and growth of voids in structural components of nuclear reactors induces dimensional instability by causing swelling, and degradation of thermal and mechanical properties resulting in the reduction of the lifetime of nuclear reactors [13–20].

The earliest models developed for studying void formation are metals used classical nucleation theory model to study the nucleation phenomenon of the voids and chemical rate theory model for void growth [14,19,20]. There are, however, three issues in the use of above classical nucleation theory for modeling the nucleation, and rate theory for void growth: firstly, nucleation and growth

are not considered simultaneously; secondly, the point defect concentrations are considered homogeneous across the solid; thirdly, the neglection of surface-controlled kinetics in the model. In structural components of nuclear reactors, voids grow simultaneously as embryos nucleate in the material [21]. The point defect production and sink terms, which are discrete in space, are homogenized across the domain in the rate theory such that the absorption of point defects by a discrete sink is the same as the absorption of the defects by a continuous sink. Moreover, the evolution equations in rate theory assume diffusion-limited kinetics. As a result, the point defects concentration is always taken to be the equilibrium values at the void interface.

Based on the preceding statements, to capture the physics of the phenomenon accurately, spatially dependent fields with point defect balances devised using principles of non-equilibrium thermodynamics [22] are required. The governing equations of the latter constitute sharp interface models. However, numerically solving the sharp interface equations requires interface tracking. Consequently, their usage was limited only to 2D problems. Therefore, phase field models [23,24] are introduced as a numerical approximation to sharp interface equations so that the tedious task of tracking the interface is replaced with an evolution equation on phase field variable. Several phase field models have been proposed to explain the void formation in irradiated metals. The governing equations of the models can be classified into either Model B or Model C [25]. In the initial models of type B formulation, the vacancy concentration field alone determines the microstructure's void evolution. Such models are known as vacancy phase field models [26–30]. Later, SIA concentration field is also considered along with vacancy field to describe the void evolution [31–33]. Nevertheless, the phase-field model of type B is limited to modeling void development in the single crystalline materials and is incapable of modeling the growth in the polycrystalline materials. However, the models of type C [34–39] drew their inspiration from the

WBM phase field model for binary alloys [40] and include an additional equation for non-conserved parameter that tracks the void evolution in the system. The phase-field formulation of type C has the capability to study the kinetics of void growth both in single crystalline and polycrystalline materials under irradiation.

All the phase field models assume that the growth kinetics are determined by the diffusion of the point defects in the matrix to the void surface. However, there exists an alternative viewpoint in the literature that the void kinetics is governed by point defect reactions at the surface. Therefore, Hochrainer and El-Azab developed a new sharp interface formulation of the void growth under irradiation that can capture the kinetics either as diffusion-controlled or as a surface-reaction controlled [41]. Aside from the differences between the two models, type B and type C, both seem to reproduce the essential details of void formation and evolution under irradiation; nevertheless, none of the phase field models match asymptotically with the sharp interface model developed by Hochrainer and El-Azab [41]. In this work, we develop a new thermodynamically consistent, quantitative phase field model of type C for void evolution that matches asymptotically with the sharp interface model.

The work is organized as follows. First, we explore in great detail the sharp interface model for void growth which is followed by a detailed derivation of the new phase field model. Then, the asymptotic analysis of the phase field model is carried out and compared with the sharp interface model. Numerical studies are presented that validate the phase-field model by comparing with the sharp interface model results, followed by concluding remarks.

II. The sharp interfacial model for void growth

Precipitation of second phase particles of a fixed concentration from a metastable solid solution is a phenomenon belonging to the class of first-order phase transitions. In particle growth, the atoms of different species are conserved, while in void growth point defects are not conserved because of recombination events wherein the point defects mutually annihilate each other. The sharp interface theory [41] developed for void formation in single component under irradiation considers a lattice framework and assumes that only isolated point defects occupy the sites of the lattice. For example, any lattice site will be occupied either by an atom, or by a vacancy, or by a self-interstitial of dumbbell type with no emphasis on the orientation of the dumbbell. Unique to this formalism is fixing the defect flux at the interface using the principles of transition state theory. The derivation of the transport equations follows the standard procedure by using the principles of non-equilibrium thermodynamics. The point defect balance equations in the matrix are given by,

$$\frac{\partial c_{\mathrm{v}}}{\partial \mathrm{t}} = -\nabla \cdot \mathbf{j_v} - R + P_{\mathrm{v}}, \tag{1}$$

$$\frac{\partial c_{\mathrm{i}}}{\partial \mathrm{t}} = -\nabla \cdot \mathbf{j_i} - R + P_{\mathrm{i}}. \tag{2}$$

In the preceding equation c_{v} and c_{i} represent the fractional concentration of the point defects in the matrix; $\mathbf{j_v}$ and $\mathbf{j_i}$ denote the flux of vacancy and self-interstitial, respectively; R represents the rate of recombination of point defects; P_{v} and P_{i} denote the source terms for vacancy and self-interstitial due to external factors, for example, irradiation. In the void, apart from $c_{\mathrm{v}} = 1$, all other quantities are taken to be zero. By neglecting surface diffusion of defects, point defect balance equations on the interface are given by [41],

$$-v[\![c_{\mathrm{v}}]\!] = -[\![\mathbf{j_v} \cdot \mathbf{n}]\!] + \sigma^{\mathrm{v}}, \tag{3}$$

$$-v[\![c_{\mathrm{i}}]\!] = -[\![\mathbf{j_i} \cdot \mathbf{n}]\!] + \sigma^{\mathrm{i}}. \tag{4}$$

In the preceding equation v denotes the scalar normal velocity of the void surface, $\mathbf{n}$ denotes the normal vector on the void surface pointing from matrix into the void; $[\![\cdot]\!]$ denotes the jump of a quantity across the surface, i.e., $[\![\cdot]\!] = \{\cdot\}_{\text{void}} - \{\cdot\}_{\text{matrix}}$; σ^{v} and σ^{i} denotes the rate of gain/loss of vacancies and self-interstitials, respectively, due to the reaction of the point defects at the void surface; $\hat{\nabla}$ is the surface del operator. Although not explicitly stated in the sharp interface model [41], $[\![\mathbf{j}_{\boldsymbol{\alpha}} \cdot \mathbf{n}]\!]$ represents the component of the total flux that preserves the identity of the defects. Here, the preservation of identity refers to the fact the defect did not annihilate after jumping the void surface. In contrast to $[\![\mathbf{j}_{\boldsymbol{\alpha}} \cdot \mathbf{n}]\!]$, the σ^{α} refers to the component of the total flux of defects where the identities are created/destroyed.

By neglecting surface diffusion of atoms, conservation of mass at a point on the surface gives the following expression for scalar normal velocity of the void surface,

$$-v[\![c_{\text{i}} - c_{\text{v}}]\!] = -[\![\mathbf{j}_{\mathbf{i}} \cdot \mathbf{n} - \mathbf{j}_{\mathbf{v}} \cdot \mathbf{n}]\!]. \tag{5}$$

Note that the source/sink terms for the point defects must be equal at the interface because annihilation or creation of a vacancy cannot take place without the corresponding annihilation or creation of a self-interstitial. A linear constitutive relation for the fluxes with their driving forces is fixed by employing the second law. The form of normal flux of point defects at the interface is obtained from the transition state theory. The normal fluxes are given by,

$$\mathbf{j}_{\mathbf{i}} \cdot \mathbf{n} = \delta \hat{c}_{\text{i}} \nu_{\text{i}} \exp\left(-\Delta g_{\text{i}}^{\text{bs}}/\text{k}_{\text{B}}\text{T}\right)\left\{1 - \exp\left[-\left(\mu_{\text{i}} - \frac{f + \Omega_{\text{a}}\kappa\gamma}{1 + c_{\text{i}} - c_{\text{v}}}\right)/\text{k}_{\text{B}}\text{T}\right]\right\}, \tag{6}$$

$$\mathbf{j}_{\mathbf{v}} \cdot \mathbf{n} = \delta \hat{c}_{\text{v}} \nu_{\text{v}} \exp\left(-\Delta g_{\text{v}}^{\text{bs}}/\text{k}_{\text{B}}\text{T}\right)\left\{1 - \exp\left[-\left(\mu_{\text{v}} + \frac{f + \Omega_{\text{a}}\kappa\gamma}{1 + c_{\text{i}} - c_{\text{v}}}\right)/\text{k}_{\text{B}}\text{T}\right]\right\}, \tag{7}$$

In the preceding equations, ν_{α}, where $\alpha = \text{i}, \text{v}$, is the attempt frequency of the point defect α; $\Delta g_{\alpha}^{\text{bs}}$ is the activation barrier which the defect must overcome to travel from the bulk to surface; δ is the distance that the surface moves per atom; f is the free energy of the defect solid at the interface;

Ω_a is the atomic volume; $\widehat{\mathbf{M}}$ is a positive definite mobility matrix; $\hat{c}_v$ and $\hat{c}_i$ represent the limiting values of the point defect concentrations at the interface on the matrix side. The expression (6) and (7) relate the normal flux of vacancy and self-interstitial, respectively, to their corresponding driving force at the void surface. Neglecting the surface diffusion of atoms and substituting the linearized expressions of equations (6) and (7) into equation (5), we obtain the following expression for the velocity of the interface:

$$v = \frac{\delta \hat{c}_v \nu_v \exp\left(-\Delta g_v^{bs}/k_B T\right)}{k_B T(\llbracket c_i - c_v \rrbracket)^2}\left(\llbracket f \rrbracket_r - \mu_v \llbracket c_v \rrbracket_r + \mu_v \llbracket c_i \rrbracket_r + \Omega_a \kappa \gamma\right) + \frac{\delta \hat{c}_i \nu_i \exp\left(-\Delta g_i^{bs}/k_B T\right)}{k_B T(\llbracket c_i - c_v \rrbracket)^2}\left(\llbracket f \rrbracket_r - \mu_i \llbracket c_i \rrbracket_r + \mu_i \llbracket c_v \rrbracket_r + \Omega_a \kappa \gamma\right), \tag{8}$$

where $\llbracket \cdot \rrbracket_r = \{\cdot\}_{matrix} - \{\cdot\}_{void}$.

The presence of activation barriers in the normal flux makes the model unique from the particle growth models. On the contrary, the models of precipitation growth aggregate all the driving forces to one force and use one mobility coefficient to relate to the velocity. In the sharp interface model for void growth, it is recognized that different driving forces in the system move the interface at different rates. Thus, the analysis of the sharp interface model for a void growth alludes to the fact that the corresponding quantitative phase field model for the void growth should possess multiple Allen-Cahn mobilities each relating the different driving forces in the system to the evolution of the phase field variable. There are two different driving forces in a void growth model which are the driving force for the reaction of a vacancy and the driving force for the reaction of a self-interstitial with the void surface. In the next section we show the derivation of a phase-field model with multiple Allen-Cahn mobilities that accurately captures the underlying physics of the void growth.

III. New phase-field model for void growth

We consider a lattice approach to model the evolution of defects in a single crystalline solid wherein each lattice site is occupied either by a vacancy, or a self-interstitial, or a regular atom, as shown in Fig. 1 [42]. The lattice density is given by $\frac{1}{\Omega_a}$, where Ω_a represents the atomic volume. Consider a sub volume V, as shown in Fig. 2, of the material system containing two phases: matrix phase with point-defects (V_+) and a void phase (V_-). The internal energy distribution and the spatial distribution of vacancies, self-interstitials, and regular atoms is described by the field variables $e(x,t)$, $c_v(x,t)$, $c_i(x,t)$ and $c_a(x,t)$ respectively. Since each lattice site can be occupied by either a vacancy, a self-interstitial, or a regular atom, there exists a lattice constraint on the field variables as follows $c_a(x,t) + c_v(x,t) + c_i(x,t) = 1$. The self-interstitials in this study are the dumbbell-type wherein two atoms share a lattice site together, while a regular atom is where a single atom entirely occupies the lattice site. No other defect clusters are considered in this study that are not voids. The void phase is defined as $c_v = 1, c_i = 0$; however, the matrix phase is not defined by any such fixed concentrations of the point defects. The phases of the system are identified by a phase-field variable $\eta(x,t)$ that takes a value of 1 in the void phase and a value of 0 in the matrix phase. Furthermore, elastic distortion of the lattice around the defects is neglected, just like in the sharp interface model.

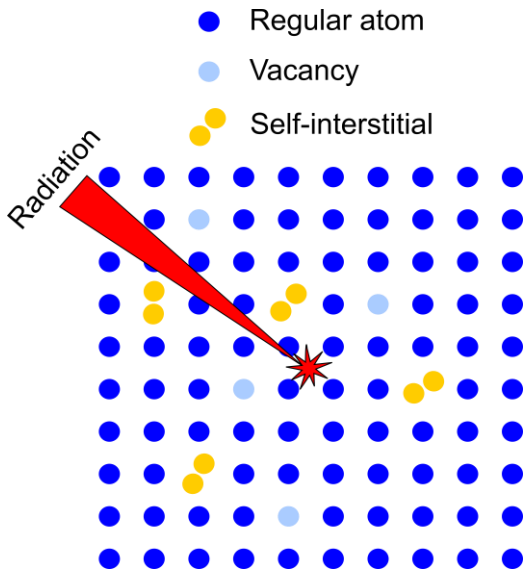

FIG. 1. Schematic of a cubic lattice depicting the typical microstructure of an irradiated single-crystalline metal with point defects.

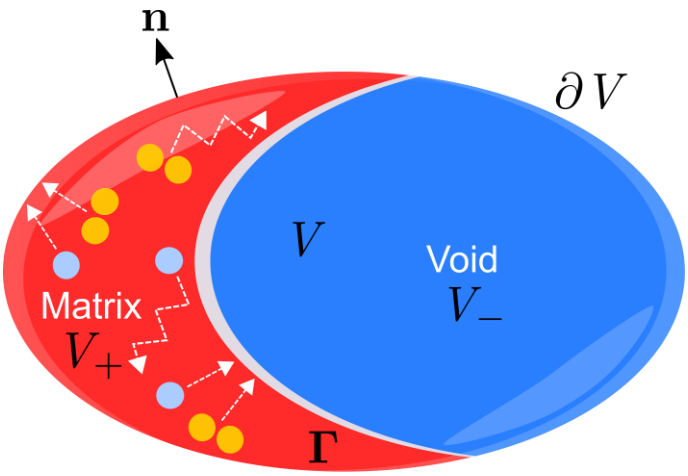

FIG. 2. Schematic of a control volume V depicting the matrix V_+ and void V_- phases separated by a diffused interface layer Γ. Here, **n** represents the normal to the boundary of the control volume ∂V. The point defects in the matrix diffuse in the matrix and some of them interact with the void or leave the control volume entirely.

A. Balance laws for internal energy and species

A thermodynamically consistent phase-field model is derived based on the balance laws for the point-defect species, energy, and entropy. Under irradiation, isolated point defects like vacancies

and self-interstitials are created as a result of displacement cascade events which supply energy in the form of heat into the material system. In addition, there is also a release of heat when the point defects annihilate each other due to the recombination events both in the bulk and at the interface. Also, heat could be conducted away from the control volume V due to a normal flux of heat at the surface of the control volume V. Combining all the statements, the energy balance equation could be written as follows:

$$\frac{1}{\Omega_{\mathrm{a}}}\frac{d}{dt}\int_V e(x,t)\,dV = -\frac{1}{\Omega_{\mathrm{a}}}\int_{\partial V}\mathbf{J_e}(x,t)\cdot\mathbf{n}\,dA + \frac{1}{\Omega_{\mathrm{a}}}\int_V \dot{q}^{\mathrm{casc}}(x,t)\,dV + \frac{1}{\Omega_{\mathrm{a}}}\int_V (-\Delta H_{\mathrm{r}})J_{\mathrm{r}}(x,t)\,dV + \frac{1}{\Omega_{\mathrm{a}}}\int_V \dot{\hat{q}}(x,t)\,dV. \tag{9}$$

In the above equation, $e(x,t)$ stands for the internal energy per lattice site, $\frac{1}{\Omega_{\mathrm{a}}}\mathbf{J_e}(x,t)\cdot\mathbf{n}$ stands for the normal flux of internal energy–with units of energy per unit area per unit time–crossing the boundary of the control volume, $\frac{1}{\Omega_{\mathrm{a}}}\dot{q}^{\mathrm{casc}}(x,t)$ represents the density of heat released due to the cascade events, $\frac{1}{\Omega_{\mathrm{a}}}J_{\mathrm{r}}(x,t)$ represents the rate of recombination of point defects per unit volume with $-\Delta H_{\mathrm{r}}$ representing the amount of energy released per one recombination event in the matrix, while $\frac{1}{\Omega_{\mathrm{a}}}\dot{\hat{q}}(x,t)$ represents the energy release rate per unit volume due to recombination of defects at the void-matrix interface and is non-zero only in the diffused interface region. Since there exists no deformation of the lattice, the volume remains fixed. As a result, from the Reynold's transport theorem, we have

$$\frac{1}{\Omega_{\mathrm{a}}}\int_V \frac{d}{dt}e(x,t)\,dV = -\frac{1}{\Omega_{\mathrm{a}}}\int_{\partial V}\mathbf{J_e}(x,t)\cdot\mathbf{n}\,dA + \frac{1}{\Omega_{\mathrm{a}}}\int_V \dot{q}^{\mathrm{casc}}(x,t)\,dV + \frac{1}{\Omega_{\mathrm{a}}}\int_V (-\Delta H_{\mathrm{r}})J_{\mathrm{r}}(x,t)\,dV + \frac{1}{\Omega_{\mathrm{a}}}\int_V \dot{\hat{q}}(x,t)\,dV. \tag{10}$$

As mentioned earlier, displacement cascade events also result in the generation of point defects in the material system. Concurrently, there is also annihilation of point defects in the material due to the recombination events both in the bulk and at the interface. Like the heat flux, a corresponding point defect flux also exists which changes the total defect content in the control volume V due to the normal flux of point defects at the surface. Therefore, the defect balance equation can be written as follows:

$$\frac{1}{\Omega_{\mathrm{a}}}\int_V \frac{d}{dt} c_\alpha(x,t)\, dV = -\frac{1}{\Omega_{\mathrm{a}}}\int_{\partial V} \mathbf{J}_{\boldsymbol{\alpha}}(x,t)\cdot \mathbf{n}\, dA + \frac{1}{\Omega_{\mathrm{a}}}\int_V P_\alpha(x,t)\, dV - \frac{1}{\Omega_{\mathrm{a}}}\int_V J_{\mathrm{r}}(x,t)\, dV + \frac{1}{\Omega_{\mathrm{a}}}\int_V \dot{\hat{g}}_\alpha(x,t)\, dV, \tag{11}$$

where $\alpha = \mathrm{i, v.}$ $\frac{1}{\Omega_{\mathrm{a}}}\mathbf{J}_{\boldsymbol{\alpha}}(x,t)\cdot\mathbf{n}$ stands for the normal flux of defects per unit area crossing the boundary of the control volume, $\frac{1}{\Omega_{\mathrm{a}}}P_\alpha(x,t)$ represents the number of defects α released per unit volume due to the cascade events, $\frac{1}{\Omega_{\mathrm{a}}}J_{\mathrm{r}}(x,t)$ represents the rate of annihilation rate of defect α per unit volume, and $\frac{1}{\Omega_{\mathrm{a}}}\dot{\hat{g}}_\alpha(x,t)$ represents the rate of defect loss/gain per unit volume and is non-zero only in the diffused interface region. Since there exists no deformation of the lattice, the volume per unit cell remains constant. Note that due to the lattice constraint, the following equations also hold true:

$$P_{\mathrm{v}}(x,t) + P_{\mathrm{i}}(x,t) + P_{\mathrm{a}}(x,t) = 0, \tag{12}$$

$$\dot{\hat{g}}_{\mathrm{v}}(x,t) + \dot{\hat{g}}_{\mathrm{i}}(x,t) + \dot{\hat{g}}_{\mathrm{a}}(x,t) = 0, \tag{13}$$

$$\mathbf{J}_{\mathbf{v}}(x,t) + \mathbf{J}_{\mathbf{i}}(x,t) + \mathbf{J}_{\mathbf{a}}(x,t) = 0. \tag{14}$$

The preceding equations are true because any lattice site should be occupied either by a vacancy, or by a self-interstitial, or by a regular atom. As a result, the evolution equation for regular atom

can be obtained from the evolution equations of the point defects. Therefore, the state of the material system can be completely specified through the independent variables $e(x,t), c_{\mathrm{v}}(x,t), c_{\mathrm{i}}(x,t)$ and $\eta(x,t)$. Removing the arguments–x, t–of the functions for brevity and assuming a periodic boundary condition at the boundary of the control volume, the following local form of balance laws can be derived using divergence theorem:

$$\dot{e}(x,t) = -\nabla \cdot \mathbf{J_e} + \dot{q}^{\mathrm{casc}} + (-\Delta H_{\mathrm{r}})J_{\mathrm{r}} + \hat{\dot{q}}, \tag{15}$$

$$\dot{c}_{\mathrm{v}}(x,t) = -\nabla \cdot \mathbf{J_v} + P_{\mathrm{v}} - J_{\mathrm{r}} + \hat{\dot{g}}_{\mathrm{v}}, \tag{16}$$

$$\dot{c}_{\mathrm{i}}(x,t) = -\nabla \cdot \mathbf{J_i} + P_{\mathrm{i}} - J_{\mathrm{r}} + \hat{\dot{g}}_{\mathrm{i}}. \tag{17}$$

Here $\dot{}$ denotes the time rate of change of the quantity.

B. Entropy functional and its balance equation

In this work, the thermodynamic state of the system is characterized through an entropy functional

$$S = \frac{1}{\Omega_{\mathrm{a}}} \int_V \left[s(e, c_{\mathrm{v}}, c_{\mathrm{i}}, \eta) - \frac{\kappa_{\eta}}{2T} |\nabla \eta|^2 \right] dV \tag{18}$$

where S is the total entropy of the control volume V; $s(e, c_{\mathrm{v}}, c_{\mathrm{i}}, \eta)$ is the local entropy density which is function of the internal energy density e, the phase-field variable η, the fractional concentration of vacancies c_{v}, and the fractional concentration of self-interstitials c_{i}. The gradient term in the entropy functional is a penalty term associated with the presence of interfaces in the system which is like the gradient terms in the free energy functional.

The time rate of change of entropy within the control volume V can be written as follows:

$$\frac{d}{dt} S = \frac{1}{\Omega_{\mathrm{a}}} \int_V \left[\frac{\partial s}{\partial e}\frac{de}{dt} + \frac{\partial s}{\partial c_{\mathrm{v}}}\frac{dc_{\mathrm{v}}}{dt} + \frac{\partial s}{\partial c_{\mathrm{i}}}\frac{dc_{\mathrm{i}}}{dt} + \frac{\partial s}{\partial \eta}\frac{d\eta}{dt} - \frac{\kappa_{\eta}}{T} \nabla \eta \cdot \nabla \dot{\eta} \right] dV. \tag{19}$$

The preceding equation can be further simplified using vector identities and divergence theorem into the following equation,

$$\frac{d}{dt}S = \frac{1}{\Omega_{\mathrm{a}}}\int_V \left[\frac{\partial s}{\partial e}\frac{de}{dt} + \frac{\partial s}{\partial c_{\mathrm{v}}}\frac{dc_{\mathrm{v}}}{dt} + \frac{\partial s}{\partial c_{\mathrm{i}}}\frac{dc_{\mathrm{i}}}{dt} + \left(\frac{\partial s}{\partial \eta} + \frac{\kappa_\eta}{T}\nabla^2\eta\right)\frac{d\eta}{dt}\right] dV - \frac{\kappa_\eta}{\Omega_{\mathrm{a}}T}\int_{\partial\mathcal{V}} \dot{\eta}\nabla\eta \cdot \mathbf{n}\, dA. \tag{20}$$

Substituting the equations (15-17) into equation (20) we get the following equation,

$$\begin{aligned}\frac{d}{dt}S = \frac{1}{\Omega_{\mathrm{a}}}\int_V \Bigg[&\frac{\partial s}{\partial e}\left(-\nabla\cdot\mathbf{J_e} + \dot{q}^{\mathrm{casc}} + (-\Delta H_{\mathrm{r}})J_{\mathrm{r}} + \dot{\hat{q}}\right) \\ &+ \frac{\partial s}{\partial c_{\mathrm{v}}}\left(-\nabla\cdot\mathbf{J_v} + P_{\mathrm{v}} - J_{\mathrm{r}} + \dot{\hat{g}}_{\mathrm{v}}\right) \\ &+ \frac{\partial s}{\partial c_{\mathrm{i}}}\left(-\nabla\cdot\mathbf{J_i} + P_{\mathrm{i}} - J_{\mathrm{r}}(x,t) + \dot{\hat{g}}_{\mathrm{i}}\right) + \left(\frac{\partial s}{\partial \eta} + \frac{\kappa_\eta}{T}\nabla^2\eta\right)\frac{d\eta}{dt}\Bigg] dV \\ &- \frac{\kappa_\eta}{\Omega_{\mathrm{a}}T}\int_{\partial V} \dot{\eta}\nabla\eta \cdot \mathbf{n}\, dA.\end{aligned} \tag{21}$$

Further simplifying the preceding equation using the vector identities and divergence theorem will result in the following equation:

$$\begin{aligned}\frac{d}{dt}S = &-\frac{1}{\Omega_{\mathrm{a}}}\int_{\partial V}\left(\frac{\kappa_\eta}{T}\dot{\eta}\nabla\eta + \mathbf{J_e}\frac{\partial s}{\partial e} + \mathbf{J_v}\frac{\partial s}{\partial c_{\mathrm{v}}} + \mathbf{J_i}\frac{\partial s}{\partial c_{\mathrm{i}}}\right)\cdot\mathbf{n}\, dA \\ &+ \frac{1}{\Omega_{\mathrm{a}}}\int_V \left[\frac{\partial s}{\partial e}\left(\dot{q}^{\mathrm{casc}} + (-\Delta H_{\mathrm{r}})J_{\mathrm{r}} + \dot{\hat{q}}\right) + \frac{\partial s}{\partial c_{\mathrm{v}}}P_{\mathrm{v}} + \frac{\partial s}{\partial c_{\mathrm{i}}}P_{\mathrm{i}}\right] dV \\ &+ \frac{1}{\Omega_{\mathrm{a}}}\int_V \Bigg[\mathbf{J_e}\cdot\nabla\left(\frac{\partial s}{\partial e}\right) + \mathbf{J_v}\cdot\nabla\left(\frac{\partial s}{\partial c_{\mathrm{v}}}\right) + \mathbf{J_i}\cdot\nabla\left(\frac{\partial s}{\partial c_{\mathrm{i}}}\right) \\ &+ \left(\frac{\partial s}{\partial \eta} + \frac{\kappa_\eta}{T}\nabla^2\eta\right)\frac{d\eta}{dt} - J_{\mathrm{r}}\left(\frac{\partial s}{\partial c_{\mathrm{v}}} + \frac{\partial s}{\partial c_{\mathrm{v}}}\right) + \frac{\partial s}{\partial c_{\mathrm{v}}}\dot{\hat{g}}_{\mathrm{v}} + \frac{\partial s}{\partial c_{\mathrm{i}}}\dot{\hat{g}}_{\mathrm{i}}\Bigg] dV.\end{aligned} \tag{22}$$

An entropy balance law could also be written like the other balance laws, considering the entropy production due to irreversible processes in the system, as following:

$$\frac{d}{dt}S = -\int_{\partial V}\mathbf{J_s}\cdot\mathbf{n}\,dA + \int_V \dot{S}^{\text{source}}\,dV + \int_V \dot{S}^{\text{prod}}\,dV. \tag{23}$$

Here, $\mathbf{J_s}$ is the entropy flux crossing the boundary of the control volume, $\dot{S}^{\text{source}}(x,t)$ is the entropy entering (or leaving) the system due to volumetric sources/sinks, and $\dot{S}^{\text{prod}}(x,t)$ is the entropy production due to irreversible processes happening within the system. By comparing the equations (22) and (23), we find that the entropy production term is of the following form:

$$\begin{aligned}\dot{S}^{\text{prod}} = \frac{1}{\Omega_\text{a}}\Bigg(&\mathbf{J_e}\cdot\nabla\left(\frac{\partial s}{\partial e}\right) + \mathbf{J_v}\cdot\nabla\left(\frac{\partial s}{\partial c_\text{v}}\right) + \mathbf{J_i}\cdot\nabla\left(\frac{\partial s}{\partial c_\text{i}}\right) + \left(\frac{\partial s}{\partial \eta} + \frac{\kappa_\eta}{T}\nabla^2\eta\right)\frac{d\eta}{dt}\\ &- J_\text{r}\left(\frac{\partial s}{\partial c_\text{v}} + \frac{\partial s}{\partial c_\text{v}}\right) + \frac{\partial s}{\partial c_\text{v}}\hat{\dot{g}}_\text{v} + \frac{\partial s}{\partial c_\text{i}}\hat{\dot{g}}_\text{i}\Bigg)\end{aligned} \tag{24}$$

Note that in the preceding equation we included the terms containing $\hat{\dot{g}}_\text{v}$ and $\hat{\dot{g}}_\text{I}$ in the entropy production term because we consider the interaction of point defects with void surface as irreversible process that leads to the evolution of the void. Moreover, as mentioned earlier, it is impossible to remove a vacancy without the removal of a self-interstitial; likewise, it is impossible to create a vacancy without creating a self-interstitial in the system. In other words, equal number of defects are created/annihilated at the void surface. Therefore, we have the following important observation, i.e.,

$$\hat{\dot{g}}_\text{v} = \hat{\dot{g}}_\text{i}. \tag{25}$$

It is possible to obtain an expression for the defect reactions at the surface if we observe that the void evolution is essentially governed by two processes: vacancy-mediated void evolution and self-interstitial-mediated void evolution. The latter statement can be expressed in an equation form as follows:

$$\dot{\eta} = \dot{\eta}_\text{v} + \dot{\eta}_\text{i}. \tag{26}$$

$\dot{\eta}_v$ represents void evolution due to vacancy-mediated process, while $\dot{\eta}_i$ represents the void evolution due to the self-interstitial-mediated process. Now, when the void evolves, either through the vacancy-mediated process or through a self-interstitial mediated process, it sweeps the defects/regular atoms ahead of the surface, as shown in Fig. 3. Thus, we note that the defect loss/gain at the interface corresponding to the void evolution at the rate of $\dot{\eta}$ should be as follows:

$$\dot{\hat{g}}_v = \dot{\hat{g}}_i = \nabla c_i \cdot \frac{\nabla\eta}{|\nabla\eta|}\frac{\dot{\eta}_v}{|\nabla\eta|} + \nabla c_v \cdot \frac{\nabla\eta}{|\nabla\eta|}\frac{\dot{\eta}_i}{|\nabla\eta|} \tag{27}$$

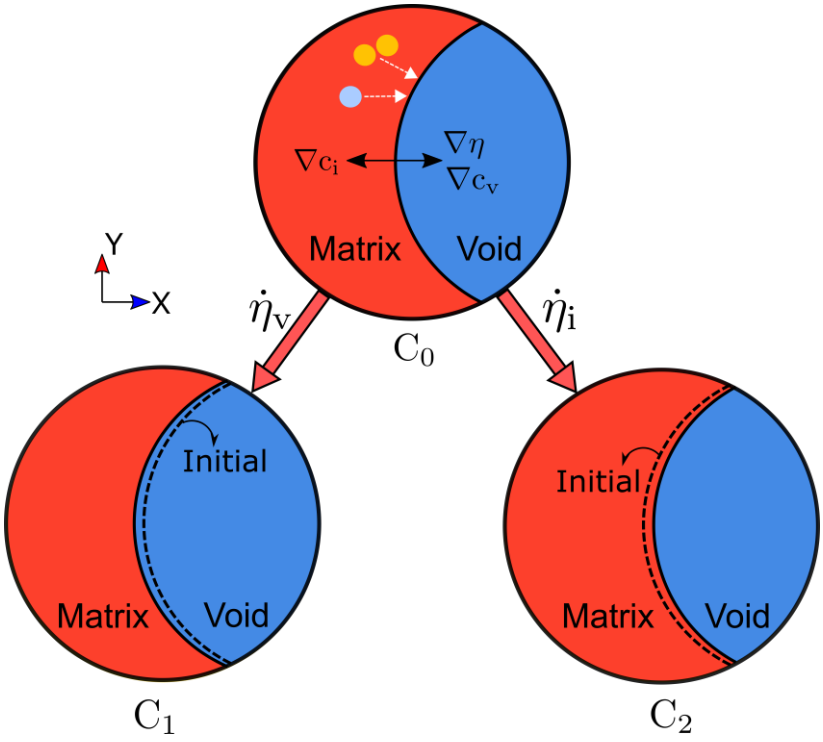

FIG. 3. Schematics illustrating the void evolution mechanisms. The arrows in C_0 represent the gradients of the field variables at the point where arrows originated. C_1 and C_2 depict the evolution of the void surface through vacancy-mediated and self-interstitial-mediated mechanisms.

The first term on the right-hand side of the preceding equation represents the number of vacancies/self-interstitials that annihilate due to the evolution of the void through a vacancy-

mediated process. The $\nabla c_{\mathrm{i}} \cdot \frac{\nabla \eta}{|\nabla \eta|}$ represents the normal gradient of the self-interstitial concentration at the void interface and $\frac{\dot{\eta}_{\mathrm{v}}}{|\nabla \eta|}$ represents the magnitude of the normal velocity of the void surface due to a vacancy-mediated process. The product, $\nabla c_{\mathrm{i}} \cdot \frac{\nabla \eta}{|\nabla \eta|} \frac{\dot{\eta}_{\mathrm{v}}}{|\nabla \eta|}$, represents the number of defects created/annihilated by the interface motion due to vacancy reactions. Likewise, the second term on the right-hand side of the equation (27) represents the number of vacancies/self-interstitials that annihilate due to the evolution of the void through a self-interstitial-mediated process. Substituting equations (26) and (27) into equation (24), we get

$$\begin{aligned} \dot{S}^{\mathrm{prod}} = \frac{1}{\Omega_{\mathrm{a}}} \Bigg[& \mathbf{J_e} \cdot \nabla \left(\frac{\partial s}{\partial e} \right) + \mathbf{J_v} \cdot \nabla \left(\frac{\partial s}{\partial c_{\mathrm{v}}} \right) + \mathbf{J_i} \cdot \nabla \left(\frac{\partial s}{\partial c_{\mathrm{i}}} \right) \\ & + \left(\frac{\partial s}{\partial \eta} + \frac{\kappa_{\eta}}{T} \nabla^2 \eta + \left(\frac{\partial s}{\partial c_{\mathrm{v}}} + \frac{\partial s}{\partial c_{\mathrm{i}}} \right) \frac{\nabla c_{\mathrm{i}} \cdot \nabla \eta}{|\nabla \eta|^2} \right) \dot{\eta}_{\mathrm{v}} \\ & + \left(\frac{\partial s}{\partial \eta} + \frac{\kappa_{\eta}}{T} \nabla^2 \eta + \left(\frac{\partial s}{\partial c_{\mathrm{v}}} + \frac{\partial s}{\partial c_{\mathrm{i}}} \right) \frac{\nabla c_{\mathrm{v}} \cdot \nabla \eta}{|\nabla \eta|^2} \right) \dot{\eta}_{\mathrm{i}} \\ & - J_{\mathrm{r}} \left(\frac{\partial s}{\partial c_{\mathrm{v}}} + \frac{\partial s}{\partial c_{\mathrm{v}}} \right) \Bigg]. \end{aligned} \tag{28}$$

However, the second law of thermodynamics states that the entropy production due to irreversible processes must be non-negative. Moreover, it is convenient to express the derivatives of the entropy density in terms of the free energy density. We know the relation between the free energy density, internal energy density and entropy density since free energy is a Legendre transform of the internal energy:

$$f(\eta, c_{\mathrm{v}}, c_{\mathrm{i}}, T) = e - Ts(e, \eta, c_{\mathrm{v}}, c_{\mathrm{i}}) \tag{29}$$

Therefore, from equation (29) we have the following relations:

$$\frac{\partial s}{\partial e} = \frac{1}{T}, \tag{30}$$

$$\frac{\partial s}{\partial c_{\mathrm{v}}} = -\frac{1}{T}\frac{\partial f}{\partial c_{\mathrm{v}}}, \tag{31}$$

$$\frac{\partial s}{\partial c_{\mathrm{i}}} = -\frac{1}{T}\frac{\partial f}{\partial c_{\mathrm{i}}}, \tag{32}$$

$$\frac{\partial s}{\partial \eta} = -\frac{1}{T}\frac{\partial f}{\partial \eta}. \tag{33}$$

The following constitutive relations for $\mathbf{J_e}$, $\mathbf{J_v}$, $\mathbf{J_i}$, $\dot{\eta}_{\mathrm{v}}$, $\dot{\eta}_i$ and J_{r} will always ensure non-negative entropy production:

$$\mathbf{J_e} = \mathbf{M_e}(c_{\mathrm{v}}, c_{\mathrm{i}}, \eta, T)\nabla\left(\frac{1}{T}\right), \tag{34}$$

$$\mathbf{J_v} = -\mathbf{M_v}(c_{\mathrm{v}}, c_{\mathrm{i}}, \eta, T)\nabla\left(\frac{1}{T}\frac{\partial f}{\partial c_{\mathrm{v}}}\right), \tag{35}$$

$$\mathbf{J_i} = -\mathbf{M_i}(c_{\mathrm{v}}, c_{\mathrm{i}}, \eta, T)\nabla\left(\frac{1}{T}\frac{\partial f}{\partial c_{\mathrm{i}}}\right), \tag{36}$$

$$\dot{\eta}_{\mathrm{v}} = -L_{\mathrm{v}}\left(\frac{\partial f}{\partial \eta} + \left(\frac{\partial f}{\partial c_{\mathrm{v}}} + \frac{\partial f}{\partial c_{\mathrm{i}}}\right)\frac{\nabla c_{\mathrm{i}} \cdot \nabla \eta}{|\nabla \eta|^2} - \kappa_{\eta}\nabla^2\eta\right), \tag{37}$$

$$\dot{\eta}_{\mathrm{i}} = -L_{\mathrm{i}}\left(\frac{\partial f}{\partial \eta} + \left(\frac{\partial f}{\partial c_{\mathrm{v}}} + \frac{\partial f}{\partial c_{\mathrm{i}}}\right)\frac{\nabla c_{\mathrm{v}} \cdot \nabla \eta}{|\nabla \eta|^2} - \kappa_{\eta}\nabla^2\eta\right), \tag{38}$$

$$J_{\mathrm{r}} = \mathrm{K}\left(\frac{\partial f}{\partial c_{\mathrm{v}}} + \frac{\partial f}{\partial c_{\mathrm{i}}}\right). \tag{39}$$

Here $\mathbf{M_e}$, $\mathbf{M_v}$, and $\mathbf{M_i}$ are positive definite mobility matrices. The mobilities of the point defects are defined as follows:

$$\mathbf{M_{\alpha}} = \frac{D_{\alpha}c_{\alpha}(1 - c_{\mathrm{v}} - c_{\mathrm{i}})}{k_{\mathrm{B}}T} \tag{40}$$

where D_{α} represents the diffusivity of the defect α, k_{B} is the Boltzmann constant and T is the temperature. In the equations (37) and (38), L_{v} and L_{i} are the positive Allen-Cahn mobility

coefficients and K is a rate constant in equation (39). Although the form selected for the recombination rate in equation (39) ensures non-negative entropy production, we use the following standard expression for the recombination rate,

$$J_{\mathrm{r}} = \mathrm{k}\left(c_{\mathrm{v}} - c_{\mathrm{v}}^{\mathrm{eqlb}}\right)\left(c_{\mathrm{i}} - c_{\mathrm{i}}^{\mathrm{eqlb}}\right), \tag{41}$$

where k is the recombination rate constant. Now the evolution equation for the phase-field variable, $\dot{\eta}$, is given by substituting the equations (37) and (38) into equation (26) and which gives the following,

$$\begin{aligned}\dot{\eta} = -L_{\mathrm{v}}\left(\frac{\partial f}{\partial \eta} + \left(\frac{\partial f}{\partial c_{\mathrm{v}}} + \frac{\partial f}{\partial c_{\mathrm{i}}}\right)\frac{\nabla c_{\mathrm{i}} \cdot \nabla \eta}{|\nabla \eta|^2} - \kappa_{\eta}\nabla^2\eta\right) \\ - L_{\mathrm{i}}\left(\frac{\partial f}{\partial \eta} + \left(\frac{\partial f}{\partial c_{\mathrm{v}}} + \frac{\partial f}{\partial c_{\mathrm{i}}}\right)\frac{\nabla c_{\mathrm{v}} \cdot \nabla \eta}{|\nabla \eta|^2} - \kappa_{\eta}\nabla^2\eta\right).\end{aligned} \tag{42}$$

The preceding equation is the modified Allen-Cahn equation that captures the evolution of the void due to vacancy-mediated and interstitial-mediated processes. This unique form of the Allen-Cahn equation has been derived for the first time using the principles of non-equilibrium thermodynamics that ensures positive entropy production for all the irreversible processes occurring in the material system, including the defect reactions with the void surfaces. Note the presence of two Allen-Cahn mobilities each relating the driving force for defect reaction to the void surface motion. The driving forces for the defect reaction contain the term $\frac{\partial f}{\partial \eta} - \kappa_{\eta}\nabla^2\eta$, which is usually found in a typical phase-field model; however, $\left(\frac{\partial f}{\partial c_{\mathrm{v}}} + \frac{\partial f}{\partial c_{\mathrm{i}}}\right)\frac{\nabla c_{\alpha} \cdot \nabla \eta}{|\nabla \eta|^2}$, where $\alpha = \mathrm{i}, \mathrm{v}$ represents the component of the driving force related to the creation/annihilation of the defects due to void surface motion. Note that $\left(\frac{\partial f}{\partial c_{\mathrm{v}}} + \frac{\partial f}{\partial c_{\mathrm{i}}}\right)\frac{\nabla c_{\mathrm{v}} \cdot \nabla \eta}{|\nabla \eta|^2}$ and $\left(\frac{\partial f}{\partial c_{\mathrm{v}}} + \frac{\partial f}{\partial c_{\mathrm{i}}}\right)\frac{\nabla c_{\mathrm{i}} \cdot \nabla \eta}{|\nabla \eta|^2}$ have different signs which is in accordance with the direction in which the vacancy and self-interstitial interactions push the

void surface. It is also fascinating to note that in the sharp interface formalism the constitutive relations are defined for the defect fluxes at the void surface, whereas in the phase-field model we define the constitutive relations for the defect source/sink terms due to the reaction with the void surface. We also note that there exists an alternative way of deriving phase-field equations which does not involve the route of first principles approach rather it is derived through reverse engineering of the sharp-interface model. It is possible to derive the equations of the phase-field model by tracing back the steps involved in the method of matched asymptotic analysis. We were able to successfully derive the phase-field equation (42) through this approach; however, the reverse engineering approach did not reveal every single detail required for deriving the equations using the principles of irreversible thermodynamics.

Nonetheless, the model is not yet quantitative because the Allen-Cahn mobility coefficients, L_{v} and L_{i}, are unknown. The application of asymptotic analysis on the phase-field model will enable us to obtain an expression of Allen-Cahn mobilities in terms of the material parameters. The asymptotic analysis of this phase-field model is shown in the succeeding section. Furthermore, we assume that interface kinetics to be orientation independent, i.e., anisotropy effects are neglected.

C. Free energy functional

The free energy functional of this inhomogeneous material system consisting of void and matrix phases is written in terms of the field variables $c_{\mathrm{v}}(x,t)$, $c_{\mathrm{i}}(x,t)$ and $\eta(x,t)$ as follows:

$$F(c_{\mathrm{v}}, c_{\mathrm{i}}, \eta, T) = \frac{1}{\Omega_{\mathrm{a}}} \int_V \left[\underbrace{f(c_{\mathrm{v}}, c_{\mathrm{i}}, \eta) + w g(\eta)}_{f(c_{\mathrm{v}}, c_{\mathrm{i}}, \eta)} + \frac{\kappa_\eta}{2} |\nabla \eta|^2 \right] dV, \tag{43}$$

where,

$$f(c_{\mathrm{v}}, c_{\mathrm{i}}, \eta) = \big(1 - h(\eta)\big)\left(f^{\mathrm{M}}(c_{\mathrm{v}}, c_{\mathrm{i}}) - f^{\mathrm{M}}\left(c_{\mathrm{v}}^{\mathrm{eqlb}}, c_{\mathrm{i}}^{\mathrm{eqlb}}\right)\right) + h(\eta) f^{\mathrm{V}}(c_{\mathrm{v}}, c_{\mathrm{i}}) \qquad (44)$$

In the preceding equation, $f^{\mathrm{M}}(c_{\mathrm{v}}, c_{\mathrm{i}})$ is the free energy per site of the matrix containing vacancies, $c_{\mathrm{v}}(x,t)$, and self-interstitials, $c_{\mathrm{i}}(x,t)$. An ideal solution form of free energy is adopted for the defected matrix, which is,

$$\begin{aligned} f^{\mathrm{M}}(c_{\mathrm{v}}, c_{\mathrm{i}}) = {} & E_{\mathrm{v}}^{\mathrm{f}} c_{\mathrm{v}} + E_{\mathrm{i}}^{\mathrm{f}} c_{\mathrm{i}} \\ & + k_{\mathrm{B}} T (c_{\mathrm{v}} \ln c_{\mathrm{v}} + c_{\mathrm{i}} \ln c_{\mathrm{i}} + (1 - c_{\mathrm{v}} - c_{\mathrm{i}}) \ln(1 - c_{\mathrm{v}} - c_{\mathrm{i}})). \end{aligned} \qquad (45)$$

In the above equation, Ω_{a} represents the atomic volume; $E_{\mathrm{v}}^{\mathrm{f}}$ and $E_{\mathrm{i}}^{\mathrm{f}}$ represent the formation energy for vacancy and a self-interstitial, respectively; k_{B} represents the Boltzmann constant and T is the temperature the inhomogeneous system. However, as it is clear from equation (44) that the free energy of the defected matrix is written with respect to the free energy of the matrix containing equilibrium concentration of point defects at the temperature T. A polynomial form of free energy expression is selected for the void phase to ensure that the concentrations of the defects remain $c_{\mathrm{v}} = 1$ and $c_{\mathrm{i}} = 0$, which is $f^{\mathrm{V}}(c_{\mathrm{v}}, c_{\mathrm{i}}) = \mathrm{a}(c_{\mathrm{v}} - 1)^2 + \mathrm{b}c_{\mathrm{i}}^2$. The void phase could be considered akin to an intermetallic compound because void phase has a fixed concentrations of point defects, which is $c_{\mathrm{v}} = 1$ and $c_{\mathrm{i}} = 0$. Since the void phase only occurs at a fixed concentration of defects, the curvature of the free energy should be very high, which could be achieved by selecting large values for the parameters a and b. For example, we have taken $\mathrm{a} = 10^4$ and $\mathrm{b} = 10^{12}$. The $h(\eta)$ is an interpolation function which interpolates the free energy between matrix and void phases at the interface. We choose the following form for the interpolation function in our work, which is, $h(\eta) = \eta^3(6\eta^2 - 15\eta + 10)$. In equation (43), $g(\eta) = \eta^2(1-\eta)^2$ is a double-well potential that ensures that the two phases, matrix phase $(\eta = 0)$ and void phase $(\eta = 1)$, are stable, while w controls the height of the double well potential but also affects the thickness of the interface. The

last term in the free energy functional is a gradient term that penalizes the system for possessing gradients in the phase-field variable and κ_η is a gradient coefficient that also affects the interface width and interfacial energy. Note that the free energy density has the units of $\mathrm{J/m^3}$, w has the units of J, while the gradient coefficient has the units of $\mathrm{J \cdot m^2}$. Also, we neglected the gradient coefficient terms corresponding to vacancies and self-interstitials, just like the KKS and grand-potential formalisms. However, the correct free energy functional should include these gradient terms because defects interact with each other locally; therefore, presence of these gradient terms for defects in the free energy functional is sensible.

IV. Asymptotic analysis

The method of matched asymptotic analysis of the phase-field model enables us to obtain a closed form expression for the Allen-Cahn mobilities and verifies whether the phase-field model is capturing the physics in the sharp interface problem [25,43,44]. Asymptotic analysis of the phase-field model examines the behavior of the model as the interface thickness is reduced. To that end, the behavior of the equations could be examined in two different limits: sharp-interface limit and thin-interface limit. In the sharp-interface limit, the equations are analyzed in the limiting case when the interface width is reduced to zero; however, in the thin-interface limit, the equations are analyzed in the limiting case when the interface width is small relative to a mesoscopic length scale defining the diffusion process. In this work, we analyzed the phase-field equations at the sharp-interface limit because the interface width is of the order of angstroms.

The idea of matched asymptotic expansion is to obtain approximate solutions to the boundary-value problem by dividing the interval into multiple sub-intervals. Then, on each sub-interval an approximate solution is constructed using the principles of perturbation theory. These approximate

solutions are then required to be matched at the overlap of each pair of sub-intervals, which gives a sequence of approximate solutions to the differential equation across the entire interval that satisfy the boundary conditions imposed on the problem. Therefore, for the material system containing the void and matrix phases, it is straightforward to divide the control volume into two sub-intervals: first, the inner region, which is the diffused interfacial region (Γ) where the state variables vary quickly across the interval; second, the outer region, where the state variables vary relatively slowly compared to the inner region, for example, the matrix V_+ and the void V_- phases. We assume that the temperature T of the material system is fixed. Therefore, the transport equations of the phase-field model that we consider are the following:

$$\dot{c}_{\mathrm{v}}(x,t) = \nabla\cdot(\boldsymbol{\mathcal{M}}_{\mathbf{v}}\nabla\mu_{\mathrm{v}}) + P_{\mathrm{v}} - J_{\mathrm{r}} + \nabla c_{\mathrm{i}}\cdot\frac{\nabla\eta}{|\nabla\eta|}\frac{\dot{\eta}_{\mathrm{v}}}{|\nabla\eta|} + \nabla c_{\mathrm{v}}\cdot\frac{\nabla\eta}{|\nabla\eta|}\frac{\dot{\eta}_{\mathrm{i}}}{|\nabla\eta|}, \tag{46}$$

$$\dot{c}_{\mathrm{i}}(x,t) = \nabla\cdot(\boldsymbol{\mathcal{M}}_{\mathbf{i}}\nabla\mu_{\mathrm{i}}) + P_{\mathrm{i}} - J_{\mathrm{r}} + \nabla c_{\mathrm{i}}\cdot\frac{\nabla\eta}{|\nabla\eta|}\frac{\dot{\eta}_{\mathrm{v}}}{|\nabla\eta|} + \nabla c_{\mathrm{v}}\cdot\frac{\nabla\eta}{|\nabla\eta|}\frac{\dot{\eta}_{\mathrm{i}}}{|\nabla\eta|}, \tag{47}$$

$$\begin{aligned}\dot{\eta} = -L_{\mathrm{v}}\left(\frac{\partial f}{\partial\eta} + w\frac{\partial g}{\partial\eta} + (\mu_{\mathrm{v}}+\mu_{\mathrm{i}})\frac{\nabla c_{\mathrm{i}}\cdot\nabla\eta}{|\nabla\eta|^2} - h\epsilon^2\nabla^2\eta\right)\\ - L_{\mathrm{i}}\left(\frac{\partial f}{\partial\eta} + w\frac{\partial g}{\partial\eta} + (\mu_{\mathrm{v}}+\mu_{\mathrm{i}})\frac{\nabla c_{\mathrm{v}}\cdot\nabla\eta}{|\nabla\eta|^2} - h\epsilon^2\nabla^2\eta\right).\end{aligned} \tag{48}$$

The gradient coefficient term in the Allen-Cahn equation is assumed to be $h\epsilon^2$, where $h = O(1)$ is a constant and ϵ is a parameter that is proportional to the interface width. As a result, the Allen-Cahn equation is a singularly perturbed equation. μ_{v} and μ_{i} represent the chemical potential of the vacancy and the self-interstitial, and $\boldsymbol{\mathcal{M}}_{\mathbf{i,v}} = \mathbf{M}_{\mathbf{i,v}}/T$. The following scaling relationships are employed for the reasons stated in [25]:

$$w \to w^{-1}\epsilon^{-1}, \tag{49}$$

$$h \to h^{-1}\epsilon^{-1}, \tag{50}$$

$$L_{\mathrm{v}} \to L_{\mathrm{v}}^{-1}\epsilon^{-1}, \tag{51}$$

$$L_{\mathrm{i}} \to L_{\mathrm{i}}^{-1}\epsilon^{-1} \tag{52}$$

Note that the superscript on ϵ is an exponent, while the superscript on w denotes the order. Consequently, the transport equations (46-48) become the following,

$$\dot{c}_{\mathrm{v}}(x,t) = \nabla\cdot(\boldsymbol{\mathcal{M}}_{\mathbf{v}}\nabla\mu_{\mathrm{v}}) + P_{\mathrm{v}} - J_{\mathrm{r}} + \frac{\nabla c_{\mathrm{i}}\cdot\nabla\eta}{|\nabla\eta|}\frac{\dot{\eta}_{\mathrm{v}}}{|\nabla\eta|} + \frac{\nabla c_{\mathrm{v}}\cdot\nabla\eta}{|\nabla\eta|}\frac{\dot{\eta}_{\mathrm{i}}}{|\nabla\eta|}, \tag{53}$$

$$\dot{c}_{\mathrm{i}}(x,t) = \nabla\cdot(\boldsymbol{\mathcal{M}}_{\mathbf{i}}\nabla\mu_{\mathrm{i}}) + P_{\mathrm{i}} - J_{\mathrm{r}} + \frac{\nabla c_{\mathrm{i}}\cdot\nabla\eta}{|\nabla\eta|}\frac{\dot{\eta}_{\mathrm{v}}}{|\nabla\eta|} + \frac{\nabla c_{\mathrm{v}}\cdot\nabla\eta}{|\nabla\eta|}\frac{\dot{\eta}_{\mathrm{i}}}{|\nabla\eta|}, \tag{54}$$

$$\begin{aligned}\epsilon\dot{\eta} = -L_{\mathrm{v}}^{-1}\left(\frac{\partial f}{\partial\eta} + w^{-1}\epsilon^{-1}\frac{\partial g}{\partial\eta} + (\mu_{\mathrm{v}}+\mu_{\mathrm{i}})\frac{\nabla c_{\mathrm{i}}\cdot\nabla\eta}{|\nabla\eta|^2} - h^{-1}\epsilon\nabla^2\eta\right)\\ - L_{\mathrm{i}}^{-1}\left(\frac{\partial f}{\partial\eta} + w^{-1}\epsilon^{-1}\frac{\partial g}{\partial\eta} + (\mu_{\mathrm{v}}+\mu_{\mathrm{i}})\frac{\nabla c_{\mathrm{v}}\cdot\nabla\eta}{|\nabla\eta|^2} - h^{-1}\epsilon\nabla^2\eta\right),\end{aligned} \tag{55}$$

with the following initial and boundary conditions,

$$c_{\mathrm{v}}(x,0) = 1, \qquad \eta(x,0) = 1, \qquad c_{\mathrm{i}} = 0, \qquad \text{for } x \in V_{-}, \tag{56}$$

$$c_{\mathrm{v}}(x,0) = C_{\mathrm{v}}(x), \qquad \eta(x,0) = 0, \qquad c_{\mathrm{i}} = C_{\mathrm{i}}(x), \qquad \text{for } x \in V_{+}, \tag{57}$$

$$\mathbf{n}\cdot\mathbf{J}_{\boldsymbol{\alpha}} = 0, \qquad \mathbf{n}\cdot\nabla c_{\alpha} = 0, \qquad \mathbf{n}\cdot\nabla\eta = 0, \qquad \text{for } x \in \partial V \text{ and } \alpha = \mathrm{i},\mathrm{v}. \tag{58}$$

In the diffused interfacial region (Γ) the variables vary smoothly from one phase to another. In addition, we assume that the initial concentrations of the point defects ensure that the matrix exists in a metastable state—leading to the void growth. Furthermore, we ensured that the terms $\frac{\nabla c_{\mathrm{v}}\cdot\nabla\eta}{|\nabla\eta|^2}$ and $\frac{\nabla c_{\mathrm{i}}\cdot\nabla\eta}{|\nabla\eta|^2}$ are non-zero only in the diffused interface region and vanish elsewhere.

In the outer region, we expand the solutions of the fields, for $\alpha = \mathrm{i},\mathrm{v}$, in the form as shown below:

$$\tilde{c}_{\alpha}(x,t) = \tilde{c}_{\alpha}^{0}(x,t) + \epsilon\tilde{c}_{\alpha}^{1}(x,t) + \epsilon^2\tilde{c}_{\alpha}^{2}(x,t) + \cdots, \tag{59}$$

$$\tilde{\eta}(x,t) = \tilde{\eta}^0(x,t) + \epsilon\tilde{\eta}^1(x,t) + \epsilon^2\tilde{\eta}^2(x,t) + \cdots, \tag{60}$$

$$\tilde{\mu}_\alpha(x,t) = \tilde{\mu}_\alpha^0(x,t) + \epsilon\tilde{\mu}_\alpha^1(x,t) + \epsilon^2\tilde{\mu}_\alpha^2(x,t) + \cdots, \tag{61}$$

$$\tilde{\mathbf{J}}_{\boldsymbol{\alpha}}(x,t) = \tilde{\mathbf{J}}_{\boldsymbol{\alpha}}^{\mathbf{0}}(x,t) + \epsilon\tilde{\mathbf{J}}_{\boldsymbol{\alpha}}^{\mathbf{1}}(x,t) + \epsilon^2\tilde{\mathbf{J}}_{\boldsymbol{\alpha}}^{\mathbf{2}}(x,t) + \cdots, \tag{62}$$

$$\widetilde{\boldsymbol{\mathcal{M}}}_{\boldsymbol{\alpha}}(x,t) = \widetilde{\boldsymbol{\mathcal{M}}}_{\boldsymbol{\alpha}}^{\mathbf{0}}(x,t) + \epsilon\widetilde{\boldsymbol{\mathcal{M}}}_{\boldsymbol{\alpha}}^{\mathbf{1}}(x,t) + \epsilon^2\widetilde{\boldsymbol{\mathcal{M}}}_{\boldsymbol{\alpha}}^{\mathbf{2}}(x,t) + \cdots, \tag{63}$$

$$\tilde{P}_\alpha(x,t) = \tilde{P}_\alpha^0(x,t) + \epsilon\tilde{P}_\alpha^1(x,t) + \epsilon^2\tilde{P}_\alpha^2(x,t) + \cdots, \tag{64}$$

$$\tilde{J}_r(x,t) = \tilde{J}_r^0(x,t) + \epsilon\tilde{J}_r^1(x,t) + \epsilon^2\tilde{J}_r^2(x,t) + \cdots. \tag{65}$$

Again, note that the superscript on ϵ is an exponent, while the superscript on the field quantities denotes the order in the perturbation series. Moreover, the Taylor series expansion of the field quantities depending on the state variables $c_\mathrm{v}, c_\mathrm{i}$ and η will result in the following relation to hold true:

$$\tilde{\mu}_\alpha^0 = \frac{\partial f(\tilde{c}_\mathrm{v}^0, \tilde{c}_\mathrm{i}^0, \tilde{\eta}^0)}{\partial \tilde{c}_\alpha}, \tag{66}$$

$$\tilde{\mu}_\alpha^1 = \sum_{\tilde{\rho}=\tilde{c}_\mathrm{v},\tilde{c}_\mathrm{i},\tilde{\eta}} \frac{\partial^2 f(\tilde{c}_\mathrm{v}^0, \tilde{c}_\mathrm{i}^0, \tilde{\eta}^0)}{\partial \tilde{c}_\alpha \partial \tilde{\rho}} \tilde{\rho}^1, \tag{67}$$

$$\widetilde{\boldsymbol{\mathcal{M}}}_{\boldsymbol{\alpha}}^{\mathbf{0}} = \widetilde{\boldsymbol{\mathcal{M}}}_{\boldsymbol{\alpha}}(\tilde{c}_\mathrm{v}^0, \tilde{c}_\mathrm{i}^0, \tilde{\eta}^0), \tag{68}$$

$$\tilde{\mathbf{J}}_{\boldsymbol{\alpha}}^{\mathbf{0}} = -\widetilde{\boldsymbol{\mathcal{M}}}_{\boldsymbol{\alpha}}^{\mathbf{0}} \nabla \tilde{\mu}_\alpha^0, \tag{69}$$

$$\tilde{P}_\alpha^0 = \tilde{P}_\alpha(\tilde{c}_\mathrm{v}^0, \tilde{c}_\mathrm{i}^0, \tilde{\eta}^0), \tag{70}$$

$$\tilde{J}_r^0 = \tilde{J}_r(\tilde{c}_\mathrm{v}^0, \tilde{c}_\mathrm{i}^0, \tilde{\eta}^0). \tag{71}$$

Now substituting the perturbation series of the various field quantities in the equations $(53-55)$ we can get different orders of the problem in the outer regions. In the case of the leading order, $O(\epsilon^{-1})$, we have

$$0 = -w^{-1}(L_\mathrm{v}^{-1} + L_\mathrm{i}^{-1}) \frac{\partial g(\tilde{\eta}^0)}{\partial \tilde{\eta}}. \tag{72}$$

For the non-zero L_{v}^{-1}, L_{i}^{-1}, and w^{-1} the only possible solution for the above equation is:

$$\tilde{\eta}^0(x,0) = 1 \ \text{ for } x \in V_-, \qquad \tilde{\eta}^0(x,0) = 0 \ \text{ for } x \in V_+. \tag{73}$$

At $O(\epsilon^0)$ we have,

$$\dot{\tilde{c}}_\alpha^0(x,t) = -\nabla \cdot \tilde{\mathbf{J}}_{\boldsymbol{\alpha}}^{\mathbf{0}} + \tilde{P}_\alpha^0 - \tilde{J}_r^0, \tag{74}$$

$$0 = -(L_{\mathrm{v}}^{-1} + L_{\mathrm{i}}^{-1})\left[w^{-1}\frac{d^2 g(\tilde{\eta}^0)}{d\tilde{\eta}^2}\tilde{\eta}^1 + \frac{\partial f(\tilde{c}_{\mathrm{v}}^0, \tilde{c}_{\mathrm{i}}^0, \tilde{\eta}^0)}{\partial \tilde{\eta}}\right] \tag{75}$$

By construction $\frac{\partial f(\tilde{c}_{\mathrm{v}}^0, \tilde{c}_{\mathrm{i}}^0, \tilde{\eta}^0)}{\partial \tilde{\eta}} = 0$ and $\frac{d^2 g(\tilde{\eta}^0)}{d\tilde{\eta}^2} \neq 0$. Therefore, we have $\tilde{\eta}^1 = 0$, which is as expected. The analysis of the equations is limited to $O(\epsilon^0)$ in the outer region. Now, we proceed to analyze the equations in the inner region.

The equations in the inner region are analyzed in a moving local orthogonal coordinate system (r, s), where r is the normal distance from any point x in the volume V to the interface $\Gamma(t)$, so that $r > 0$ implies that the point x lies in V_+ and $r < 0$ implies that the point x lies in V_-. s represents the two coordinates perpendicular to r which are tangent to the interface $\Gamma(t)$. In this moving coordinate system, the normal to the interface, curvature and the velocity of the interface are defined in the following way:

$$\mathbf{m} = \nabla r, \qquad \kappa = \nabla \cdot \mathbf{m} = \nabla^2 r, \qquad v = -\frac{\partial r}{\partial t} \tag{76}$$

In the preceding equation, $\mathbf{m}$ represents the normal to the interface $\Gamma(t)$ facing towards V_+; κ represents the mean curvature of the interface $\Gamma(t)$, which takes a positive sign when the center of the curvature lies in V_-; finally, v represents the normal velocity of the interface, positive when the interface is moving towards V_+. Furthermore, we introduce a stretched variable $z = \frac{r}{\epsilon}$. In the moving orthogonal coordinate system (z, s) the transport equations (46-48) transform as follows:

$$\epsilon^2 \frac{\partial c_\alpha}{\partial t}\left(\frac{\partial \eta}{\partial z}\right)^2 - \epsilon v \frac{\partial c_\alpha}{\partial z}\left(\frac{\partial \eta}{\partial z}\right)^2$$

$$= \frac{\partial\left(\boldsymbol{\mathcal{M}}_{\boldsymbol{\alpha}} \frac{\partial \mu_\alpha}{\partial z}\right)}{\partial z}\left(\frac{\partial \eta}{\partial z}\right)^2 + \epsilon \boldsymbol{\mathcal{M}}_{\boldsymbol{\alpha}} \kappa \frac{\partial \mu_\alpha}{\partial z}\left(\frac{\partial \eta}{\partial z}\right)^2 + \epsilon^2 \nabla_{\mathrm{s}}$$

$$\cdot \left(\boldsymbol{\mathcal{M}}_{\boldsymbol{\alpha}} \nabla_{\mathrm{s}} \mu_\alpha\right)\left(\frac{\partial \eta}{\partial z}\right)^2 + \epsilon^2 P_\alpha \left(\frac{\partial \eta}{\partial z}\right)^2 - \epsilon^2 J_{\mathrm{r}} \left(\frac{\partial \eta}{\partial z}\right)^2$$

$$- L_{\mathrm{v}}^{-1}\left(\epsilon \frac{\partial f}{\partial \eta}\frac{\partial \eta}{\partial z} + w^{-1}\frac{\partial g}{\partial \eta}\frac{\partial \eta}{\partial z} + \epsilon(\mu_{\mathrm{v}} + \mu_{\mathrm{i}})\frac{\partial c_{\mathrm{i}}}{\partial z}\right. \tag{77}$$

$$\left. - h^{-1}\left(\frac{\partial^2 \eta}{\partial z^2} + \epsilon\kappa\frac{\partial \eta}{\partial z} + \epsilon^2 \nabla_{\mathrm{s}}^2 \eta\right)\right)\frac{\partial c_{\mathrm{i}}}{\partial z}$$

$$- L_{\mathrm{i}}^{-1}\left(\epsilon \frac{\partial f}{\partial \eta}\frac{\partial \eta}{\partial z} + w^{-1}\frac{\partial g}{\partial \eta}\frac{\partial \eta}{\partial z} + \epsilon(\mu_{\mathrm{v}} + \mu_{\mathrm{i}})\frac{\partial c_{\mathrm{v}}}{\partial z}\right.$$

$$\left. - h^{-1}\left(\frac{\partial^2 \eta}{\partial z^2} + \epsilon\kappa\frac{\partial \eta}{\partial z} + \epsilon^2 \nabla_{\mathrm{s}}^2 \eta\right)\right)\frac{\partial c_{\mathrm{v}}}{\partial z},$$

$$\epsilon \frac{\partial \eta}{\partial t}\frac{\partial \eta}{\partial z} - v\left(\frac{\partial \eta}{\partial z}\right)^2$$

$$= -L_{\mathrm{v}}^{-1}\left(\frac{\partial f}{\partial \eta}\frac{\partial \eta}{\partial z} + w^{-1}\epsilon^{-1}\frac{\partial g}{\partial \eta}\frac{\partial \eta}{\partial z} + (\mu_{\mathrm{v}} + \mu_{\mathrm{i}})\frac{\partial c_{\mathrm{i}}}{\partial z}\right.$$

$$\left. - h^{-1}\left(\epsilon^{-1}\frac{\partial^2 \eta}{\partial z^2}\frac{\partial \eta}{\partial z} + \kappa\left(\frac{\partial \eta}{\partial z}\right)^2 + \epsilon\nabla_{\mathrm{s}}^2 \eta \frac{\partial \eta}{\partial z}\right)\right) \tag{78}$$

$$- L_{\mathrm{i}}^{-1}\left(\frac{\partial f}{\partial \eta}\frac{\partial \eta}{\partial z} + w^{-1}\epsilon^{-1}\frac{\partial g}{\partial \eta}\frac{\partial \eta}{\partial z} + (\mu_{\mathrm{v}} + \mu_{\mathrm{i}})\frac{\partial c_{\mathrm{v}}}{\partial z}\right.$$

$$\left. - h^{-1}\left(\epsilon^{-1}\frac{\partial^2 \eta}{\partial z^2}\frac{\partial \eta}{\partial z} + \kappa\left(\frac{\partial \eta}{\partial z}\right)^2 + \epsilon\nabla_{\mathrm{s}}^2 \eta \frac{\partial \eta}{\partial z}\right)\right).$$

Note that $\frac{\partial \eta}{\partial s} = 0$ because the value of η does not change on surface at fixed r. An analogy explaining $\frac{\partial \eta}{\partial s} = 0$ could be taking a surface derivative of η on a level set representing a fixed value of η.

In the inner regions, the fields are expanded in the perturbation series of the following form:

$$c_\alpha(x,t) = c_\alpha^0(x,t) + \epsilon c_\alpha^1(x,t) + \epsilon^2 c_\alpha^2(x,t) + \cdots, \tag{79}$$

with similar expressions for the various other field quantities. At this stage, it is important to introduce matching conditions that both inner and outer solutions satisfy at the overlap of the regions. Given any field quantity ϕ defined on the domain V and let x be any point on the interface $\Gamma(t)$, we require the following condition to hold at the boundary of the two regions:

$$\left(\tilde{\phi}^0 + \epsilon\tilde{\phi}^1 + \cdots\right)(x + \epsilon z\mathbf{m}) = (\phi^0 + \epsilon\phi^1 + \cdots)(z,s,t). \tag{80}$$

Applying Taylor series expansion on the left and matching the expression of the same order on both sides will gives us the following matching conditions:

$$\phi^0(z = \pm\infty, s, t) = \tilde{\phi}^0(r = \pm 0, s, t), \tag{81}$$

$$\phi^1(z = \pm\infty, s, t) = \tilde{\phi}^1(r = \pm 0, s, t) + z\frac{\partial \phi^0(r = \pm 0, s, t)}{\partial r}, \tag{82}$$

$$\begin{aligned}\phi^2(z = \pm\infty, s, t) = \tilde{\phi}^2(r = \pm 0, s, t) + z\frac{\partial \phi^1(r = \pm 0, s, t)}{\partial r} \\ + \frac{1}{2}z^2\frac{\partial^2 \phi^0(r = \pm 0, s, t)}{\partial r^2}.\end{aligned} \tag{83}$$

Substituting the perturbation series of the field quantities into the phase-field equations, for $O(\epsilon^{-1})$, we have,

$$0 = \left(w^{-1} \frac{\partial g(\eta^0)}{\partial \eta} - h^{-1} \frac{\partial^2 \eta^0}{\partial z^2} \right) \frac{\partial \eta^0}{\partial z}. \tag{84}$$

Since η^0 cannot be a constant across the diffused interface, we get the following equation from the above equation:

$$0 = w^{-1} \frac{\partial g(\eta^0)}{\partial \eta} - h^{-1} \frac{\partial^2 \eta^0}{\partial z^2}. \tag{85}$$

The preceding equation is a Euler-Lagrange equation that gives the equilibrium profile for the field η^0 satisfying the conditions $\eta^0(z = +\infty) = 0$ and $\eta^0(z = -\infty) = 1$. For the next leading order $O(\epsilon^0)$, we have the following equations:

$$\begin{aligned} 0 = {} & \frac{\partial \left(\boldsymbol{\mathcal{M}}_{\alpha}^{0} \frac{\partial \mu_{\alpha}^{0}}{\partial z} \right)}{\partial z} \left(\frac{\partial \eta^0}{\partial z} \right)^2 \\ & - \left(w^{-1} \frac{\partial g(\eta^0)}{\partial \eta} - h^{-1} \frac{\partial^2 \eta^0}{\partial z^2} \right) \left[L_{\mathrm{v}}^{-1} \frac{\partial c_{\mathrm{i}}^0}{\partial z} + L_{\mathrm{i}}^{-1} \frac{\partial c_{\mathrm{v}}^0}{\partial z} \right]. \end{aligned} \tag{86}$$

$$\begin{aligned} -v \left(\frac{\partial \eta^0}{\partial z} \right)^2 = {} & -L_{\mathrm{v}}^{-1} \left(\frac{\partial f(c_{\mathrm{v}}^0, c_{\mathrm{i}}^0, \eta^0)}{\partial \eta} \frac{\partial \eta^0}{\partial z} + w^{-1} \frac{\partial^2 g(\eta^0)}{\partial \eta^2} \eta^1 \frac{\partial \eta^0}{\partial z} \right. \\ & \left. + (\mu_{\mathrm{v}}^0 + \mu_{\mathrm{i}}^0) \frac{\partial c_{\mathrm{i}}^0}{\partial z} - h^{-1} \kappa \left(\frac{\partial \eta^0}{\partial z} \right)^2 - h^{-1} \frac{\partial^2 \eta^1}{\partial z^2} \frac{\partial \eta^0}{\partial z} \right) \\ & - L_{\mathrm{i}}^{-1} \left(\frac{\partial f(c_{\mathrm{v}}^0, c_{\mathrm{i}}^0, \eta^0)}{\partial \eta} \frac{\partial \eta^0}{\partial z} + w^{-1} \frac{\partial^2 g(\eta^0)}{\partial \eta^2} \eta^1 \frac{\partial \eta^0}{\partial z} \right. \\ & \left. + (\mu_{\mathrm{v}}^0 + \mu_{\mathrm{i}}^0) \frac{\partial c_{\mathrm{v}}^0}{\partial z} - h^{-1} \kappa \left(\frac{\partial \eta^0}{\partial z} \right)^2 - h^{-1} \frac{\partial^2 \eta^1}{\partial z^2} \frac{\partial \eta^0}{\partial z} \right). \end{aligned} \tag{87}$$

From equation (85) and using the fact that $\frac{\partial \eta^0}{\partial z}$, $\frac{\partial c_{\mathrm{i}}^0}{\partial z}$ and $\frac{\partial c_{\mathrm{v}}^0}{\partial z}$ are non-zero, equation (86) becomes,

$$\mu_{\alpha}^{0} = A_{\alpha}(s, t). \tag{88}$$

Now, integrating the equation (87) from $z = -\infty$ to $z = +\infty$, we get the following relation,

$$-v\int_{-\infty}^{+\infty}\left(\frac{\partial\eta^0}{\partial z}\right)^2 dz$$

$$= -L_{\mathrm{v}}^{-1}\int_{-\infty}^{+\infty}\left(\frac{\partial f(c_{\mathrm{v}}^0,c_{\mathrm{i}}^0,\eta^0)}{\partial\eta}\frac{\partial\eta^0}{\partial z}+w^{-1}\frac{\partial^2 g(\eta^0)}{\partial\eta^2}\eta^1\frac{\partial\eta^0}{\partial z}\right.$$

$$\left.+(\mu_{\mathrm{v}}^0+\mu_{\mathrm{i}}^0)\frac{\partial c_{\mathrm{i}}^0}{\partial z}-h^{-1}\kappa\left(\frac{\partial\eta^0}{\partial z}\right)^2-h^{-1}\frac{\partial^2\eta^1}{\partial z^2}\frac{\partial\eta^0}{\partial z}\right)dz \qquad (89)$$

$$-L_{\mathrm{i}}^{-1}\int_{-\infty}^{+\infty}\left(\frac{\partial f(c_{\mathrm{v}}^0,c_{\mathrm{i}}^0,\eta^0)}{\partial\eta}\frac{\partial\eta^0}{\partial z}+w^{-1}\frac{\partial^2 g(\eta^0)}{\partial\eta^2}\eta^1\frac{\partial\eta^0}{\partial z}\right.$$

$$\left.+(\mu_{\mathrm{v}}^0+\mu_{\mathrm{i}}^0)\frac{\partial c_{\mathrm{v}}^0}{\partial z}-h^{-1}\kappa\left(\frac{\partial\eta^0}{\partial z}\right)^2-h^{-1}\frac{\partial^2\eta^1}{\partial z^2}\frac{\partial\eta^0}{\partial z}\right)dz.$$

However, one can show the following relation to be true,

$$\int_{-\infty}^{+\infty}\left(w^{-1}\frac{\partial^2 g(\eta^0)}{\partial\eta^2}\eta^1\frac{\partial\eta^0}{\partial z}-h^{-1}\frac{\partial^2\eta^1}{\partial z^2}\frac{\partial\eta^0}{\partial z}\right)dz=0. \qquad (90)$$

Along with equation (90) and the following equality,

$$\frac{df(c_{\mathrm{v}}^0,c_{\mathrm{i}}^0,\eta^0)}{dz}=\frac{\partial f(c_{\mathrm{v}}^0,c_{\mathrm{i}}^0,\eta^0)}{\partial c_{\mathrm{v}}}\frac{\partial c_{\mathrm{v}}^0}{\partial z}+\frac{\partial f(c_{\mathrm{v}}^0,c_{\mathrm{i}}^0,\eta^0)}{\partial c_{\mathrm{i}}}\frac{\partial c_{\mathrm{i}}^0}{\partial z}+\frac{\partial f(c_{\mathrm{v}}^0,c_{\mathrm{i}}^0,\eta^0)}{\partial\eta}\frac{\partial\eta^0}{\partial z}, \qquad (91)$$

equation (89) will reduce to the dynamical Gibbs-Thompson equation of the following:

$$v=L_{\mathrm{v}}\delta\left(\left[\!\left[f(\tilde{c}_{\mathrm{v}}^0,\tilde{c}_{\mathrm{i}}^0,\tilde{\eta}^0)\right]\!\right]_{\mathrm{r}}-\tilde{\mu}_{\mathrm{v}}^0\left[\!\left[\tilde{c}_{\mathrm{v}}^0\right]\!\right]_{\mathrm{r}}+\tilde{\mu}_{\mathrm{v}}^0\left[\!\left[\tilde{c}_{\mathrm{i}}^0\right]\!\right]_{\mathrm{r}}-\kappa\gamma_{\eta}\right)$$
$$+L_{\mathrm{i}}\delta\left(\left[\!\left[f(\tilde{c}_{\mathrm{v}}^0,\tilde{c}_{\mathrm{i}}^0,\tilde{\eta}^0)\right]\!\right]_{\mathrm{r}}-\tilde{\mu}_{\mathrm{i}}^0\left[\!\left[\tilde{c}_{\mathrm{i}}^0\right]\!\right]_{\mathrm{r}}+\tilde{\mu}_{\mathrm{i}}^0\left[\!\left[\tilde{c}_{\mathrm{v}}^0\right]\!\right]_{\mathrm{r}}-\kappa\gamma_{\eta}\right). \qquad (92)$$

In the preceding equation, $\gamma_{\eta}=\int_{-\infty}^{+\infty}h\epsilon\left(\frac{\partial\eta^0}{\partial z}\right)^2 dz$ is the surface energy, while $\delta={h\epsilon^2}/{\gamma_{\eta}}$ is the diffuse interface width, which is of the order of the surface layer thickness as stated in [25]. Note that the form of the dynamical Gibbs-Thompson equation (92) matches exactly with velocity

expression derived in sharp-interface model, except that the sign ahead of curvature term is opposite. In the sharp interface model, curvature term is positive when the center of the curvature lies in V_+, which is in complete contrast with the definition of curvature in the phase-field model. The comparison not only confirms that the phase-field model captures the physics of the problem, but also provides the following relations for the Allen-Cahn mobility terms:

$$L_{\mathrm{v}} = \frac{\hat{c}_{\mathrm{v}}\nu_{\mathrm{v}}\exp\left(-\Delta g_{\mathrm{v}}^{\mathrm{bs}}/k_{\mathrm{B}}\mathrm{T}\right)}{k_{\mathrm{B}}\mathrm{T}(\llbracket c_{\mathrm{i}} - c_{\mathrm{v}} \rrbracket)^2} \cong \frac{\hat{c}_{\mathrm{v}}\nu_{\mathrm{v}}\exp\left(-\Delta g_{\mathrm{v}}^{\mathrm{bs}}/k_{\mathrm{B}}\mathrm{T}\right)}{k_{\mathrm{B}}\mathrm{T}}, \tag{93}$$

$$L_{\mathrm{i}} = \frac{\hat{c}_{\mathrm{i}}\nu_{\mathrm{i}}\exp\left(-\Delta g_{\mathrm{i}}^{\mathrm{bs}}/k_{\mathrm{B}}\mathrm{T}\right)}{k_{\mathrm{B}}\mathrm{T}(\llbracket c_{\mathrm{i}} - c_{\mathrm{v}} \rrbracket)^2} \cong \frac{\hat{c}_{\mathrm{i}}\nu_{\mathrm{i}}\exp\left(-\Delta g_{\mathrm{i}}^{\mathrm{bs}}/k_{\mathrm{B}}\mathrm{T}\right)}{k_{\mathrm{B}}\mathrm{T}}. \tag{94}$$

Thus, all the parameters, except w and κ_η are fixed in the phase-field model bringing the model closer to being a predictive phase-field model. Furthermore, higher order analysis will give us the jump balance conditions for the point defects and a higher order correction to the dynamical Gibbs-Thompson condition, which we do not show here.

V. Model verification

A. Non-dimensionalization and the numerical approach

The kinetic equations for the state variables $c_{\mathrm{v}}, c_{\mathrm{i}}$ and η, which are given in eqns. $(46-48)$, are reduced to a non-dimensionalized form that makes the values of the parameters more or less of the same order which aids in numerically solving them with ease. The spatial distances are scaled by a distance l and time is scaled by τ, while the energies are scaled by $k_{\mathrm{B}}T$. As a result, the transport equations are reduced to the following form:

$$\frac{\partial c_{\mathrm{v}}}{\partial \bar{t}} = \bar{\nabla}\cdot(\overline{\boldsymbol{\mathcal{M}}}_{\mathrm{v}}\bar{\nabla}\bar{\mu}_{\mathrm{v}}) + \bar{P}_{\mathrm{v}} - \bar{J}_{\mathrm{r}} + \bar{\nabla}c_{\mathrm{i}}\cdot\frac{\bar{\nabla}\eta}{|\bar{\nabla}\eta|}\frac{\dot{\bar{\eta}}_{\mathrm{v}}}{|\bar{\nabla}\eta|} + \bar{\nabla}c_{\mathrm{v}}\cdot\frac{\bar{\nabla}\eta}{|\bar{\nabla}\eta|}\frac{\dot{\bar{\eta}}_{\mathrm{i}}}{|\bar{\nabla}\eta|}, \tag{95}$$

$$\frac{\partial c_{\mathrm{i}}}{\partial \bar{t}} = \bar{\nabla} \cdot (\overline{\boldsymbol{\mathcal{M}}}_{\mathbf{i}} \bar{\nabla} \bar{\mu}_{\mathrm{i}}) + \bar{P}_{\mathrm{i}} - \bar{J}_{\mathrm{r}} + \bar{\nabla} c_{\mathrm{i}} \cdot \frac{\bar{\nabla}\eta}{|\bar{\nabla}\eta|} \frac{\dot{\bar{\eta}}_{\mathrm{v}}}{|\bar{\nabla}\eta|} + \bar{\nabla} c_{\mathrm{v}} \cdot \frac{\bar{\nabla}\eta}{|\bar{\nabla}\eta|} \frac{\dot{\bar{\eta}}_{\mathrm{i}}}{|\bar{\nabla}\eta|}, \tag{96}$$

$$\begin{aligned} \frac{\partial \eta}{\partial \bar{t}} = &-\bar{L}_{\mathrm{v}} \left(\frac{\partial \bar{f}}{\partial \eta} + \bar{w} \frac{\partial g}{\partial \eta} + (\bar{\mu}_{\mathrm{v}} + \bar{\mu}_{\mathrm{i}}) \frac{\bar{\nabla} c_{\mathrm{i}} \cdot \bar{\nabla}\eta}{|\bar{\nabla}\eta|^2} - \bar{\kappa}_{\eta} \bar{\nabla}^2 \eta \right) \\ &- \bar{L}_{\mathrm{i}} \left(\frac{\partial \bar{f}}{\partial \eta} + \bar{w} \frac{\partial g}{\partial \eta} + (\bar{\mu}_{\mathrm{v}} + \bar{\mu}_{\mathrm{i}}) \frac{\bar{\nabla} c_{\mathrm{v}} \cdot \bar{\nabla}\eta}{|\bar{\nabla}\eta|^2} - \bar{\kappa}_{\eta} \bar{\nabla}^2 \eta \right). \end{aligned} \tag{97}$$

In the preceding equation, $\bar{\nabla} = l\nabla$, $t = \tau \bar{t}$, $\bar{P}_{\alpha} = \tau P_{\alpha}$, $\bar{J}_r = \tau J_r$, $\bar{w} = {}^{w}/_{k_{\mathrm{B}} T \bar{\Omega}_{\mathrm{a}}}$, $\bar{\kappa}_{\eta} = {}^{\kappa_{\eta}}/_{l^2 k_{\mathrm{B}} T \bar{\Omega}_{\mathrm{a}}}$, $\bar{\mu}_{\alpha} = {}^{\mu_{\alpha}}/_{k_{\mathrm{B}} T \bar{\Omega}_{\mathrm{a}}}$, $\bar{f} = {}^{f}/_{k_{\mathrm{B}} T \bar{\Omega}_{\mathrm{a}}}$, $\overline{\boldsymbol{\mathcal{M}}}_{\boldsymbol{\alpha}} = {}^{D_{\alpha} c_{\alpha} \tau \bar{\Omega}_{\mathrm{a}}}/_{l^2}$ and $\bar{L}_{\alpha} = L_{\alpha} \tau \bar{\Omega}_{\mathrm{a}} k_{\mathrm{B}} T$. Note that in the latter equations $\bar{\Omega}_{\mathrm{a}}$ is a scalar constant that has the same magnitude as that of atomic volume, Ω_{a}, but is dimensionless.

TABLE I. Material parameters.

Parameter	Value	Units
T	1000	K
γ	1.65	$\mathrm{J/m^2}$
$E_{\mathrm{v}}^{\mathrm{f}}$	0.98	eV
$E_{\mathrm{i}}^{\mathrm{f}}$	2.2	eV
Ω_{a}	12	$\mathrm{Å^3}$
$\nu_{\mathrm{i/v}}$	72300	$\mathrm{ns^{-1}}$
$E_{\mathrm{v}}^{\mathrm{m}}$	0.8	eV
$E_{\mathrm{i}}^{\mathrm{m}}$	0.24	eV
D_{v}	0.23	$\mathrm{nm^2/ns}$
D_{i}	12.34	$\mathrm{nm^2/ns}$

The values of the material and the model parameters are listed in Table I and Table II, respectively. We have chosen the element Cu for our test cases. In this work, we have taken a fixed, isotropic value for the mobility of the defects. The mobility values are calculated at $T = 1000$ K using the material parameters stated in Table I. The mobility parameter requires the

knowledge of spatial dependent concentration of defects; however, we have assumed for all the simulations an average concentration as follows: $\langle c_{\mathrm{v}} \rangle = 10^{-4}$ and $\langle c_{\mathrm{i}} \rangle = 10^{-6}$. Since the concentration of the defects at the interface is impossible to estimate in the phase-field models, we used nominal values to estimate the Allen-Cahn mobility coefficients: $\hat{c}_{\mathrm{v}} = 10^{-5}$ and $\hat{c}_{\mathrm{i}} = 10^{-10}$. To obtain estimates for the Landau coefficient (w) and the gradient coefficient (κ_{η}), we used the KKS formalism [45] by introducing additional variables defining the concentration variables in the phases, followed by the constraints on those new variables. The activation barriers, $\Delta g_{\mathrm{v}}^{\mathrm{bs}}$ and $\Delta g_{\mathrm{i}}^{\mathrm{bs}}$, are assumed to be the same as the migration barriers of the defects in the matrix. Finally, we considered the equilibrium interface thickness to be 2 nm.

TABLE II. Model parameters.

Parameter	Value
$\overline{\boldsymbol{\mathcal{M}}}_{\mathbf{v}}$	2.7
$\overline{\boldsymbol{\mathcal{M}}}_{\mathbf{i}}$	1.4
$\bar{L}_{\mathrm{v}}$	57.9
$\bar{L}_{\mathrm{i}}$	0.4
$\bar{w}$	1054
$\bar{\kappa}_{\eta}$	244
τ	10^7
l	1

These equations are solved using the finite element method in MOOSE framework. Multiphysics object–oriented simulation environment—or MOOSE, is an open–source, parallel finite element framework—is developed and maintained by Idaho National Laboratory. In this work, unless otherwise specified, we have chosen to work with a 2D simulation domain of size $200\ \mathrm{nm} \times 200\ \mathrm{nm}$. The source terms and the bulk recombination terms are turned off. We discretized the spatial domain using quadrilateral elements with linear Lagrange shape functions.

Mesh adaptivity was employed with three levels of mesh refinement, where at the finest level of refinement $\Delta x = \Delta y = 0.18$ nm. A zero flux boundary condition is used in all the directions. A second-order accurate backward differentiation formula was used as a time-integrator alongside an IterationAdaptiveDT time stepper [46,47]. We used an absolute convergence tolerance of 10^{-6} for our simulations.

B. Gibbs-Thompson effect

We first show, using the vacancy phase-field model, that the model captures the Gibbs-Thompson effect, in other words, the curvature effect. For this we chose to work with a simulation domain of size 80 nm $\times$ 80 nm. Voids of different radii are initialized at the center of the simulation domain with the initial concentration of vacancy in the matrix is set to 10^{-4}. The simulations are run long enough till there are no fluctuations in the size of the void. In the Table III, we report the initial radius, equilibrium concentration computed by the classical nucleation theory for a given size of the void, equilibrium vacancy concentration computed by the vacancy phase-field model, and the final radius of the void at equilibrium. The phase-field model clearly captures the Gibbs-Thompson effect whereby the equilibrium vacancy concentration in the matrix decreases with the increase in the size of the void; however, the values are off by a slight extent which could be attributed to the numerical errors.

Furthermore, we also tested the model to see if it demonstrates the Ostwald ripening effect when there are voids of different radii close to each other. In this case, we chose to work with the full phase-field model that considers both vacancies and self-interstitials, as detailed in the earlier sections. Two voids of radii 6 nm and 12 nm are initialized at the center domain with a separation distance of 22 nm between the centers of the void. The vacancy concentration in the matrix is initialized to equilibrium concentration. It is clear from Fig. 4 that with increase in time the smaller

void shrinks by releasing vacancies into the matrix, while the larger void expands by absorbing those vacancies. The underlying cause for the latter phenomenon is the Gibbs-Thompson effect. In the beginning, the chemical potential of a vacancy at the surface of the smaller void is greater than a vacancy chemical potential inside the matrix, thus causing the smaller void to release vacancies into the matrix. Also, the chemical potential of a vacancy at the surface of a larger void is greater than the chemical potential of a vacancy in the matrix, but smaller than the chemical potential of a vacancy at the surface of a smaller void, causing the larger void to release vacancies into the matrix too. Eventually, a concentration gradient develops across the space between the voids that leads to the diffusion of vacancies from the smaller void to the larger void leading to the shrinkage and disappearance of the smaller void.

TABLE 3. Equilibrium vacancy concentration for different void radii.

Radius (nm)	c_v^{eq} (CNT)	c_v^{eq} (Phase-field)	Final Radius (nm)
6	1.14×10^{-5}	1.45×10^{-5}	5.99
8	1.07×10^{-5}	1.37×10^{-5}	7.98
10	1.04×10^{-5}	1.32×10^{-5}	9.98
12	1.01×10^{-5}	1.29×10^{-5}	12.0

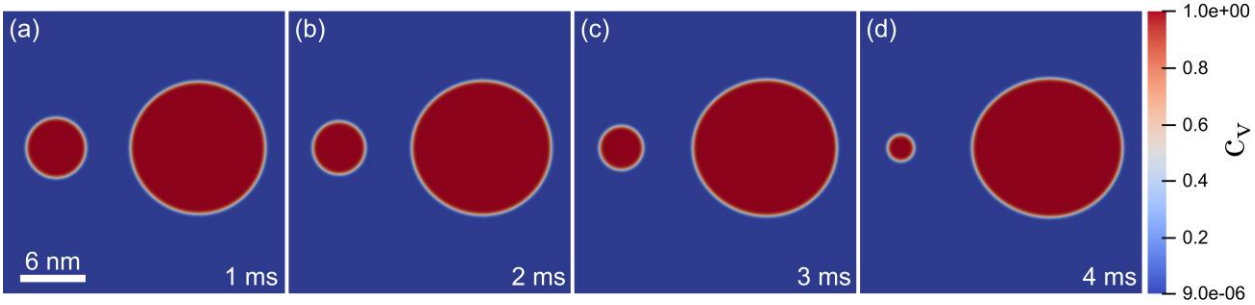

FIG. 4. Phase-field simulation depicting the Ostwald ripening phenomenon. Two voids of initial diameter 6 nm and 12 nm are initialized at the center of a simulation domain of size 200 nm × 200 nm which are separated by 22 nm across the centers of the void. The initial concentration of the vacancies in the matrix is set to the equilibrium value.

C. Kinetics

The real test of the new phase-field involves comparing the evolution of the void at a given temperature and at a given supersaturation of defects with the evolution predicted by the sharp interface. In these set of test cases, we select a 2D simulation domain of size $200\ \text{nm} \times 200\ \text{nm}$ with a void of radius 8 nm initialized at the center of the simulation domain. Different supersaturations of the defects are considered in the matrix and the evolution of the void predicted by the sharp interface model and the phase-field model is reported in Fig. 4. The parameters used in the phase-field model are reported in Table I. The evolution equations of the sharp-interface model are solved in the manner described in [41]. Figure 5 indicates that the phase-field model is reasonably accurate in predicting the evolution of the void. The absolute difference between the radius of the void predicted by the sharp-interface and phase-field model is of the order of angstrom. Thus, we have a new phase-field that is capable of quantitatively predicting the evolution of the void in a defect supersaturated environment.

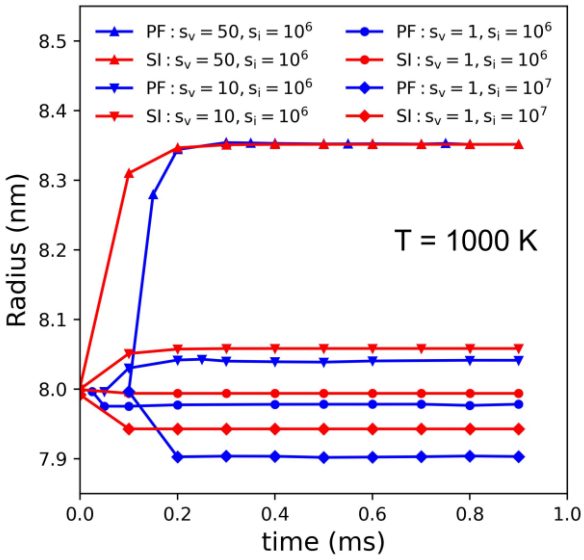

FIG. 5. Evolution of the void under various defect supersaturation environments predicted by the sharp-interface and phase-field model at 1000 K. The initial size of the void is set to 8 nm. Here

s_v and s_i refer to the supersaturation of vacancy and self-interstitial defects with respect to their equilibrium values, respectively.

VI. Conclusion

In this work, we developed a thermodynamically consistent, quantitative diffuse interface model based on KKS formalism to describe the void evolution under defect supersaturated environments. The model concurrently considers both vacancies and self-interstitials in the description of void evolution. In this new phase-field model, we successfully captured the defect reaction asymmetry with the void surface by deriving an Allen-Cahn equation with two Allen-Cahn mobilities. Each Allen-Cahn mobility relates the driving force for the defect reaction with the evolution of the phase-field variable. The asymptotic matching of the phase-field model with the sharp-interface theory fixed the two mobility parameters in terms of the material parameters in the sharp-interface model. The Landau coefficient, which controls the height of the double-well function in the phase field variable, and the gradient coefficient of the phase field variable are fixed based on the interfacial energy and interface width of the boundary. The model captures the Gibbs-Thompson effect both through the radius dependent equilibrium vacancy concentration and through the successful demonstration of the Ostwald ripening effect. Furthermore, the single void evolution kinetics captured by the phase-field model closely traces that of the sharp-interface model depicting the successful capture of the physics of the void evolution in our phase-field model. With all the parameters in the model determined in terms of the material parameters, we thus have a quantitative phase field model for void evolution with predictive capability.

Acknowledgements

We acknowledge the financial support by NSF-CMMI-1728419. We would also like to acknowledge Prof. Thomas Hochrainer for providing us with the code to solve the equations of the sharp-interface model.

References

[1] C. Fan, A. R. G. Sreekar, Z. Shang, J. Li, M. Li, H. Wang, A. El-Azab, and X. Zhang, *Radiation Induced Nanovoid Shrinkage in Cu at Room Temperature: An in Situ Study*, Scr Mater **166**, 112 (2019).

[2] T. Niu et al., *In Situ Study on Heavy Ion Irradiation Induced Microstructure Evolution in Single Crystal Cu with Nanovoids at Elevated Temperature*, Mater Today Commun **33**, (2022).

[3] X. Fan, Cuncai; Annadanam, Rayaprolu Goutham Sreekar; Shang, Zhongxia; Li, Jin; Li, Meimei; Wang, Haiyan; El-Azab, Anter; Zhang, *Irradiation Induced Void Spheroidization, Shrinkage and Migration in Cu at Elevated Temperature: An in Situ Study*, Acta Mater (n.d.).

[4] T. Niu, M. Nasim, R. G. S. Annadanam, C. Fan, J. Li, Z. Shang, Y. Xue, A. El-Azab, H. Wang, and X. Zhang, *Recent Studies on Void Shrinkage in Metallic Materials Subjected to In Situ Heavy Ion Irradiations*, JOM **72**, 4008 (2020).

[5] H. Mehl, O. Biham, O. Millo, and M. Karimi, *Electromigration-Induced Flow of Islands and Voids on the Cu(001) Surface*, Phys Rev B Condens Matter Mater Phys **61**, 4975 (2000).

[6] D. N. Bhate, A. Kumar, and A. F. Bower, *Diffuse Interface Model for Electromigration and Stress Voiding*, J Appl Phys **87**, 1712 (2000).

[7] L. Baňas and R. Nürnberg, *Phase Field Computations for Surface Diffusion and Void Electromigration in $\mathbb{R}3$*, Comput Vis Sci **12**, 319 (2009).

[8] D. R. Fridline and A. F. Bower, *Influence of Anisotropic Surface Diffusivity on Electromigration Induced Void Migration and Evolution*, J Appl Phys **85**, 3168 (1999).

[9] B. Chao, S. H. Chae, X. Zhang, K. H. Lu, M. Ding, J. Im, and P. S. Ho, *Electromigration Enhanced Intermetallic Growth and Void Formation in Pb-Free Solder Joints*, J Appl Phys **100**, (2006).

[10] V. Borovikov and M. I. Mendelev, *Void Growth via Dislocation Pileup Impingement on Grain Boundary*, Mater Lett **291**, 129542 (2021).

[11] W. D. Yang, X. Wang, and G. Lu, *The Evolution of Void Defects in Metallic Films Based on a Nonlocal Phase Field Model*, Eng Fract Mech **127**, 12 (2014).

[12] Y. Tao, F. Kong, Z. Li, J. Zhang, X. Zhao, Q. Yin, D. Xing, and P. Li, *A Review on Voids of 3D Printed Parts by Fused Filament Fabrication*, Journal of Materials Research and Technology.

[13] T. K. GUPTA, *Instability of Cylindrical Voids in Alumina*, Journal of the American Ceramic Society **61**, 191 (1978).

[14] K. C. Russell, *Nucleation of Voids in Irradiated Metals*, Acta Metallurgica **19**, 753 (1971).

[15] BULLOUGH R, EYRE BL, and PERRIN RC, *Growth and Stability of Voids in Irradiated Metals*, Nucl Appl Technol **9**, 346 (1970).

[16] K. Krishan, *ORDERING OF VOIDS AND GAS BUBBLES IN RADIATION ENVIRONMENTS.*, Radiat Eff **66**, 121 (1982).

[17] J. L. Katz and H. Wiedersich, *Nucleation of Voids in Materials Supersaturated with Vacancies and Interstitials*, J Chem Phys **55**, 1414 (1971).

[18] A. You, M. A. Y. Be, and I. In, *Nucleation of Voids in Materials Supersaturated with Vacancies and Interstitials*, **1414**, (2015).

[19] R. M. Mayer and L. M. Brown, *Nucleation and Growth of Voids by Radiation: I. Formulation of the Problem*, Journal of Nuclear Materials **95**, 46 (1980).

[20] H. Wiedersich, *On the Theory of Void Formation during Irradiation*, Http://Dx.Doi.Org/10.1080/00337577208231128 **12**, 111 (2006).

[21] G. S. Was, *Fundamentals of Radiation Materials Science: Metals and Alloys* (springer, 2016).

[22] G. Lebon, D. Jou, J. Casas-Vázquez Foundations, and F. Lebon, Understanding Non-Equilibrium Understanding Non-Equilibrium Thermodynamics, n.d.

[23] I. Steinbach, *Phase-Field Models in Materials Science*, Model Simul Mat Sci Eng **17**, (2009).

[24] D. Tourret, H. Liu, and J. Llorca, *Progress in Materials Science Phase-Field Modeling of Microstructure Evolution : Recent Applications , Perspectives and Challenges*, Prog Mater Sci **123**, 100810 (2022).

[25] Karim Ahmed and A. El-Azab, *An Analysis of Two Classes of Phase Field Models for Void Growth and Coarsening in Irradiated Crystalline Solids*, Materials Theory **2**, 1 (2018).

[26] A. A. Semenov and C. H. Woo, *Interfacial Energy in Phase-Field Emulation of Void Nucleation and Growth*, Journal of Nuclear Materials **411**, 144 (2011).

[27] A. A. Semenov and C. H. Woo, *Phase-Field Modeling of Void Formation and Growth under Irradiation*, Acta Mater **60**, 6112 (2012).

[28] Z. H. Xiao, A. A. Semenov, C. H. Woo, and S. Q. Shi, *Single Void Dynamics in Phase Field Modeling*, Journal of Nuclear Materials (2013).

[29] S. Y. Hu and C. H. Henager, *Phase-Field Simulation of Void Migration in a Temperature Gradient*, Acta Mater **58**, 3230 (2010).

[30] H. C. Yu and W. Lu, *Dynamics of the Self-Assembly of Nanovoids and Nanobubbles in Solids*, Acta Mater **53**, 1799 (2005).

[31] A. A. Semenov and C. H. Woo, *Modeling Void Development in Irradiated Metals in the Phase-Field Framework*, Journal of Nuclear Materials (2014).

[32] Y. Li, S. Hu, X. Sun, F. Gao, C. H. Henager, and M. Khaleel, *Phase-Field Modeling of Void Evolution and Swelling in Materials under Irradiation*, in *Science China: Physics, Mechanics and Astronomy* (2011).

[33] S. Hu and C. H. Henager, *Phase-Field Modeling of Void Lattice Formation under Irradiation*, Journal of Nuclear Materials **394**, 155 (2009).

[34] S. Rokkam, A. El-Azab, P. Millett, and D. Wolf, *Phase Field Modeling of Void Nucleation and Growth in Irradiated Metals*, Model Simul Mat Sci Eng **17**, (2009).

[35] A. El-Azab, K. Ahmed, S. Rokkam, and T. Hochrainer, *Diffuse Interface Modeling of Void Growth in Irradiated Materials. Mathematical, Thermodynamic and Atomistic Perspectives*, Curr Opin Solid State Mater Sci **18**, 90 (2014).

[36] N. Wang, S. Rokkam, T. Hochrainer, M. Pernice, and A. El-Azab, *Asymptotic and Uncertainty Analyses of a Phase Field Model for Void Formation under Irradiation*, Comput Mater Sci **89**, 165 (2014).

[37] P. C. Millett, A. El-Azab, S. Rokkam, M. Tonks, and D. Wolf, *Phase-Field Simulation of Irradiated Metals*, Comput Mater Sci **50**, 949 (2010).

[38] P. C. Millett, A. El-Azab, S. Rokkam, M. Tonks, and D. Wolf, *Phase-Field Simulation of Irradiated Metals*, Comput Mater Sci **50**, 949 (2011).

[39] P. C. Millett, S. Rokkam, A. El-Azab, M. Tonks, and D. Wolf, *Void Nucleation and Growth in Irradiated Polycrystalline Metals: A Phase-Field Model*, Model Simul Mat Sci Eng **17**, (2009).

[40] A. A. Wheeler, W. J. Boettinger, and G. B. McFadden, *Phase-Field Model of Solute Trapping during Solidification*, Phys Rev E **47**, 1893 (1993).

[41] T. Hochrainer and A. El-Azab, *A Sharp Interface Model for Void Growth in Irradiated Materials*, Philosophical Magazine **95**, 948 (2015).

[42] S. Rokkam, Phase Field Modeling of Void Nucleation and Growth in Irradiated Materials, Ph. D. Dissertation, Florida State University, 2011.

[43] E. S. Nani and B. Nestler, *Asymptotic Analysis of Multi-Phase-Field Models: A Thorough Consideration of Junctions*, Phys Rev E **107**, (2023).

[44] E. S. Nani and B. Nestler, *Asymptotic Analysis of Multi-Phase-Field Models: A Thorough Consideration of Binary Interfaces*, Phys Rev E **105**, (2022).

[45] S. G. Kim, W. T. Kim, and T. Suzuki, Phase-Field Model for Binary Alloys, 1999.

[46] C. J. Permann et al., *MOOSE: Enabling Massively Parallel Multiphysics Simulation*, SoftwareX **11**, (2020).

[47] D. Schwen, L. K. Aagesen, J. W. Peterson, and M. R. Tonks, Rapid Multiphase-Field Model Development Using a Modular Free Energy Based Approach with Automatic Differentiation in MOOSE/MARMOT, 2017.